Science Bulletin 65 (2020) 70–88

Contents lists available at ScienceDirect

Science Bulletin

journal homepage: www.elsevier.com/locate/scib

Science Bulletin
www.scibull.com

Review

Recent progress in tactile sensors and their applications in intelligent systems

Yue Liu [a,c,1], Rongrong Bao [a,c,d,1], Juan Tao [a,c], Jing Li [a,c], Ming Dong [e], Caofeng Pan [a,b,c,d,*]

[a] CAS Center for Excellence in Nanoscience, Beijing Key Laboratory of Micro-nano Energy and Sensor, Beijing Institute of Nanoenergy and Nanosystems, Chinese Academy of Sciences, Beijing 100083, China
[b] College of Physics and Optoelectronic Engineering, Shenzhen University, Shenzhen 518060, China
[c] School of Nanoscience and Technology, University of Chinese Academy of Sciences, Beijing 100049, China
[d] Center on Nanoenergy Research, School of Physical Science and Technology, Guangxi University, Nanning 530004, China
[e] Beijing Institute of Tracking and Telecommunications Technology, Beijing 100094, China

ARTICLE INFO

Article history:
Received 21 August 2019
Received in revised form 19 September 2019
Accepted 9 October 2019
Available online 22 October 2019

Keywords:
Tactile sensor
Intelligent system
Self-powered capability
Biodegradability
Self-healing

ABSTRACT

With the rapid development of intelligent technology, tactile sensors as sensing devices constitute the core foundation of intelligent systems. Biological organs that can sense various stimuli play vital roles in the interaction between human beings and the external environment. Inspired by this fact, research on skin-like tactile sensors with multifunctionality and high performance has attracted extensive attention. An overview of the development of high-performance tactile sensors applied in intelligent systems is systematically presented. First, the development of tactile sensors endowed with stretchability, self-healing, biodegradability, high resolution and self-powered capability is discussed. Then, for intelligent systems, tactile sensors with excellent application prospects in many fields, such as wearable devices, medical treatment, artificial limbs and robotics, are presented. Finally, the future prospects of tactile sensors for intelligent systems are discussed.

1. Introduction

The development and application of intelligent systems have significantly improved the quality of people's lives and provided great convenience in many aspects [1]. For example, recent wearable intelligent systems can collect large amounts of data at any time to determine illness [2]. At the same time, intelligent systems for human–computer interaction have been widely used in robots, electronic tablets, biometric devices, etc. [3–7]. However, intelligent systems that work in complex environments require precise coordination of various sensors. Among them, tactile sensors are the most important and complex sensors because they can be used to construct a large-area fast-response high-resolution system [8–10]. As shown in Fig. 1, tactile sensors have been already used in every aspect of daily life, and their high performance has been well studied by researchers, such as high-resolution, stretchability, self-healing, self-powered capability and biodegradability. Among them, high resolution promotes the development of human–computer interaction interface and robotics. Stretchability makes devices more similar to human skin and extends the range of application of tactile sensors. Self-healing greatly increases the service life of the devices. Self-powered capability realizes the collection of natural energy, and biodegradability provides a development direction for transient electronics. Intelligent systems made up of these tactile sensors are gradually changing the way people live and work, and with the progress of science and technology, people's ideas will change dramatically. The tactile organs of most animals are all over their body [24] and exhibit various sensing capabilities, such as for temperature, humidity, mechanical stimulation and roughness [25–28]. Faced with the application requirements of wearable electronic devices and devices used in the biomedical field, human–computer interaction, intelligent robotics and other fields, tactile sensors are needed not only to mimic the tactile organs of human skin but also to express sensations in a quantitative way [29]. Therefore, realizing this functionality has been one of the important challenges and bottlenecks in the field of sensors for a long time [30].

Broadly speaking, for application in intelligent systems, tactile sensors possessing high performance refer to flexible electronic devices, which are generally made of lightweight, stretchable and elastic materials [31]. According to the working mechanism, tactile sensors are mainly based on the piezoelectric, capacitive, and

* Corresponding author.
E-mail address: cfpan@binn.cas.cn (C. Pan).
[1] These authors contributed equally to this work

https://doi.org/10.1016/j.scib.2019.10.021
2095-9273/

Fig. 1. (Color online) High performance of different tactile sensors applied in intelligent systems. High resolution: a tactile sensor matrix was used for visualized sensing and real-time tactile mapping. Reprinted with permission from Refs. [11,12], Copyright © 2016 Wiley-VCH. Stretchability: tactile sensors based on flexible materials or stretchable structures were used for sensing a variety of stimuli, such as temperature, humidity and stress. Reprinted with permission from Refs. [13–15], Copyright © 2018 Wiley-VCH, © 2018 Springer Nature. Self-healing: tactile sensors can repair themselves because of the interaction between the special covalent bonds or supramolecular bonds, which can extend the service life of tactile sensors. Reprinted with permission from Refs. [16,17], Copyright © 2012, Springer Nature, © 2018 American Chemical Society. Self-powered: nanogenerators, as tactile sensors based on the piezoelectric or triboelectric effect, were used for tactile perception without an external energy source. Reprinted with permission from Refs. [18,19], Copyright © 2017 Wiley-VCH, © 2018 Elsevier. Biodegradability: tactile sensors based on natural or synthetic materials, such as silk protein and PLGA, can be implanted in the body, and they degrade under certain conditions. Reprinted with permission from Refs. [20–23], Copyright © 2012 AAAS, © 2016, 2019 Springer Nature, © 2017 National Academy of Sciences.

piezoresistive effects. Among them, the piezoelectric effect refers to the electric polarization of a piezoelectric material caused by a mechanical force [32]. Tactile sensors based on the piezoelectric effect have the advantages of high natural frequency, high sensitivity, high signal-to-noise ratio and good stability [33]. As for capacitive tactile sensors, whose operating principle is that the variation in the capacitance depends on the change in the relative position between the plates under an external pressure, they can be integrated over a large area and used at low power consumption [34]. The piezoresistive tactile sensors based on the piezoresistive effect, in which the conductivity varies under an external pressure, have the advantages of large detection, simple signal processing, and strong anti-interference capability compared with other types of sensors [35]. In addition to the three types of tactile sensors

mentioned above, photoelectric, photoelectromagnetic, and magnetoresistive sensors are also applied in many fields for intelligent systems [36].

In the early days of the development of tactile sensors, studies about touch were limited to whether the sensor was in contact with the object or the degree of contact [36]. Followed by great efforts, more detailed works on the design, principles and methods of sensors were conducted to improve their performance [37]. To date, tactile sensors with high performance have been an essential element in intelligent systems. In the operation process of an intelligent system, tactile sensors are used to transform the physical, chemical and biological information acquired by direct sensing perception into digital information, which can be easily recognized and transmitted to the back-end platform for processing and analysis. As a typical example, Takashima and co-workers [25,38] designed a piezoelectric three-dimensional force tactile sensor, which was installed on the end of the smart finger of a robot. Marcus Meyer of Germany developed an octopus-like underwater robot with a new tactile system that accurately sensed obstacle conditions and automatically performed surveys of the seabed environment [39]. The new hairy electronic skin developed by Seoul National University in Korea can be widely used in prosthetics, heart rate monitors and robots [40].

In this review, we first focus on the development of tactile sensors with high performance, mainly high resolution, stretchability, self-healing, self-powered capability and biodegradability. Then, great potential applications in intelligent systems based on the tactile sensors with high performance are presented, such as wearable electronic devices, devices in the biomedical field, human–computer interaction systems and intelligent robots. Finally, we summarize the breakthroughs made in recent years in tactile sensors and outline the future development of tactile sensors for intelligent systems.

2. High-performance sensors

The high performance of tactile sensors has driven their development in intelligent systems. Many efforts have been made to develop new tactile sensor functionalities to satisfy different applications in intelligent systems. Material selection and structure design play important roles in achieving good performance and various functions [41]. In this section, we mainly introduce several tactile sensors based on new materials and structures that achieved high performance in intelligent systems. First, high resolution is one of the prime performance parameters of tactile sensors. The introduction of the piezotronic and piezo-phototronic effects ensures tactile sensors with high resolution. For further adaption to intelligent systems, on the basis of these two effects, new materials have been utilized to enable flexible tactile sensors under the premise of a high resolution. Second, to mimic human skin, stretchability is an essential feature for tactile sensors to realize the personification of intelligent systems. Therefore, intrinsically stretchable materials and stretchable structures are used to provide tactile sensors with stretchability. Third, tactile sensors will inevitably encounter mechanical injury in ordinary operation. Self-healing is an important function when the devices are damaged and cannot work properly. The combination of covalent adaptive bonds and supramolecular noncovalent bonds makes devices self-healing. Fourth, a self-powered capability means that tactile sensors no longer have to rely on external batteries, which enables devices with not only decreased size but also reduced natural energy consumption. Piezoelectric and triboelectric nanogenerators used as tactile sensors provide the foundation for self-powered devices. Finally, with the increasing awareness of environmental protection and the increasing needs of medicine, the biodegradability of tactile sensors plays a significant role in intelligent systems. Specific inorganic materials can endow devices with the ability to self-degrade in the environment, but some features limit their development in intelligent systems. To meet more application scenarios, breakthroughs have been made in the field of organic materials.

2.1. High resolution

Electronic devices with high resolution facilitate the development of robotics and human–machine interfaces. A high resolution enables accurate identification of the position and direction of objects by robots so that they can flexibly complete the task [42]. Additionally, tactile sensors with high resolution can effectively identify the appearance of complex objects in low visibility environments [43]. Therefore, this capability is necessary for tactile sensors to be used in electronic skin, imaging systems, intelligent signature systems and other applications.

However, ordinary piezoresistive or capacitive pressure sensors still have limited resolution of millimeter magnitude. Encouragingly, the piezotronic effect was used to improve resolution. The piezotronic effect arises as a result of the polarization of nonmobile ions in the crystal. It is an interface effect that asymmetrically modulates local contacts at different terminals of the device because of the polarity of the piezoelectric potential. The principle of strain-gated piezoelectric transistor is different from that of conventional field-effect transistors. It is realized on the metal–semiconductor contact interface through strain-induced ion polarization charge modulation local contact characteristics and carrier transport, so the piezotronic effect can improve the resolution of tactile sensors greatly. On the basis of the piezotronic effect, Wang group [44] prepared a taxel-addressable pressure/force sensor composed of a plurality of vertical ZnO nanowires between upper and lower electrodes. A schematic diagram of the device is displayed in Fig. 2a. Each nanowire was strained by an axial pressure. Because polarized nonflowing ions were distributed at both ends, a piezoelectric potential was generated inside the nanowire. When pressure was applied to taxels 45 and 46, an obvious and steady response could be observed, as shown in Fig. 2b. The introduction of the piezotronic effect into tactile sensors not only improved the resolution of devices but also extended some potential applications in intelligent systems. As shown in Fig. 2c, this group successfully realized an integrated 92×92 taxel strain-gated vertical piezotronic transistor (SGVPT) array. The two-dimensional current contour plot shows that the currents of the SGVPTs were very consistent. To prove the tactile sensitivity, this group pressed a die onto the device with a pressure of approximately 25 kPa. Different pressures showed different current values, and the two-terminal transistor array exhibited high resolution [44].

In addition, for visualization, the piezo-phototronic effect has been introduced to convert a force signal into an optical signal and reduce the resolution to the micron scale. Our group [45] developed a sensor array based on nanowire light-emitting diodes (LEDs) with a two-dimensional distribution of stress mapping. n-ZnO nanowires were patterned on a p-GaN substrate to form a pixeled light-emitting array, as shown in Fig. 2d. Each pixel consisted of a single n-ZnO nanowire/p-GaN LED. As shown in Fig. 2e, f, this device had an extremely high spatial resolution of 2.7 μm, which corresponded to a pixel density of 6350 dpi. The recovery time of the pressure sensor was fast, approximately 90 ms. Due to the piezo-phototronic effect, the local strain on the device determined the light emission density of each pixel. Afterwards, a "piezo" model on a sapphire substrate was used as a seal on the LED array to detect the distribution of two-dimensional strain. The light-emitting image for a strain of −0.15% applied to the device clearly

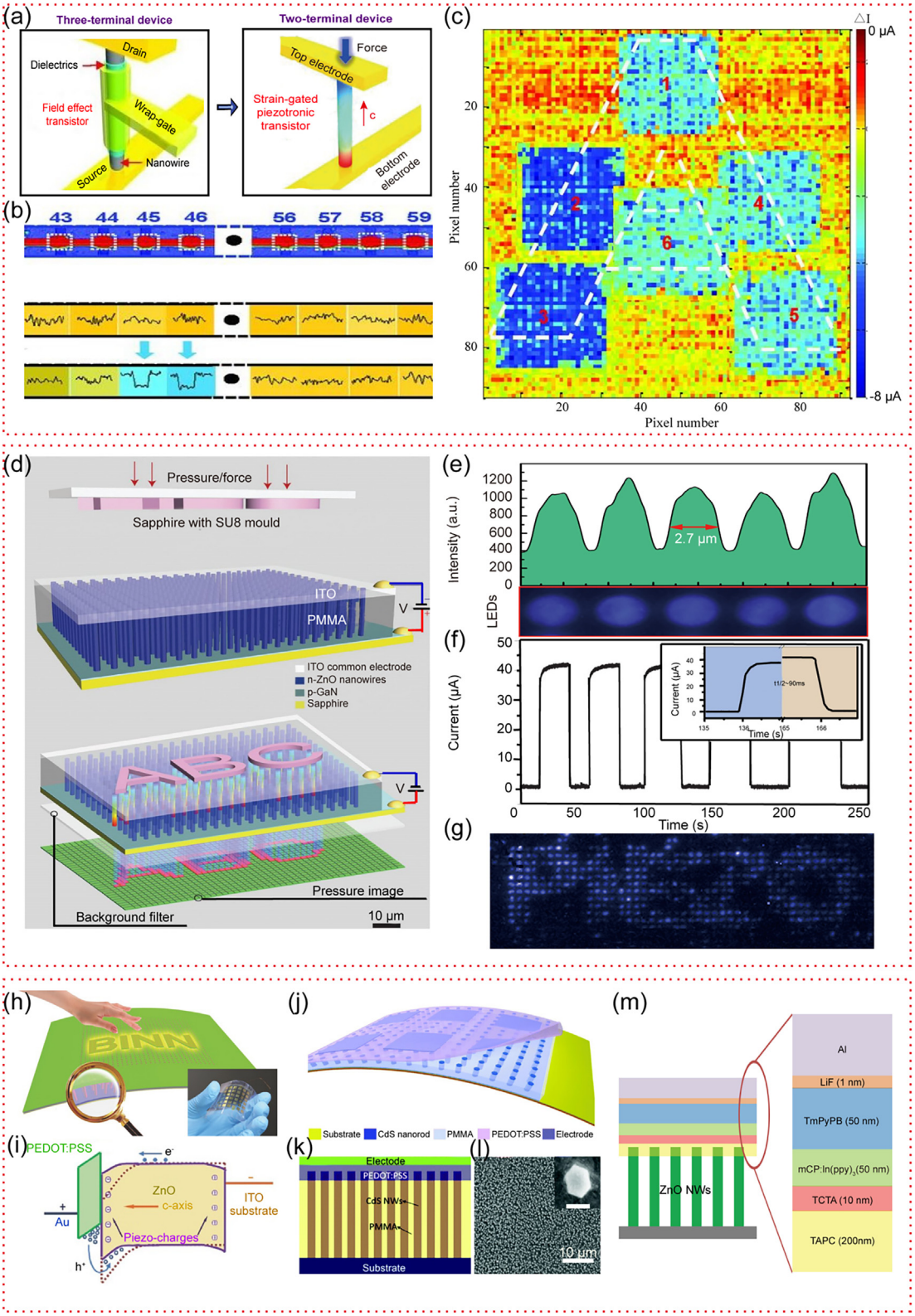

Fig. 2. (Color online) High resolution of devices. SGVPT: schematic diagram of a three-terminal device and a two-terminal device (a), the response of taxels 45 and 46 to pressure (b), and tactile imaging by the fully integrated 92 × 92 SGVPT array (c). Reprinted with permission from Ref. [44], Copyright © 2013 AAAS. n-ZnO NW/p-GaN LED array based on the piezo-phototronic effect: schematic of the LED array exhibiting a pressure distribution (d), the resolution of the LED array was 2.7 μm (e), the recovery time of the pressure sensor was approximately 90 ms (f), and the LED array exhibited a stress distribution in the pattern "PIEZO" (g). Reprinted with permission from Ref. [45], Copyright © 2013 Springer Nature. (h–m) Flexible high-resolution sensors based on traditional and new materials: flexible ZnO NW/p-polymer LED array based on the piezo-phototronic effect (h, i), flexible CdS nanorod/organic hybrid LED array based on the piezo-phototronic effect (the inset bar is 200 nm) (j–l), and flexible ZnO NW/OLED array based on the piezotronic effect (m). Reprinted with permission from Refs. [46–48], Copyright © 2015 Wiley-VCH, © 2016, 2019 RSC, © 2017 American Chemical Society.

showed the word "piezo" with little crosstalk between adjacent pixels, as shown in Fig. 2g. Then, to further mimic human skin and enable adaption to intelligent systems, new materials, for example, ZnO, GaN and CdS NWs, were used to provide a way to simultaneously achieve flexibility and high resolution of sensors [49–51]. Based on the piezo-phototronic effect, our group [46] prepared a flexible LED array with ZnO NWs and p-polymer to achieve pressure mapping, as shown in Fig. 2h, i. Bao and co-workers [47] fabricated a PN junction, which consisted of CdS nanorods and organic layers grown on indium tin oxide (ITO) electrodes by the hydrothermal method, and they prepared an LED array based on the piezo-phototronic effect for mapping the pressure. A schematic diagram of the device is shown in Fig. 2j, k. The distribution of pressure had a high spatial resolution of 1.5 μm. The recombination of electron holes at the device interface determined its luminescence intensity. Fig. 2l shows an scanning electron microscope (SEM) image of the CdS nanorods; their tops were dipped into a poly(methyl methacrylate) (PMMA) layer. Bao et al. [48] designed an array that combines ZnO nanowires with organic LEDs. As shown in Fig. 2m, the light emission performance was determined by the organic luminescent layer. In addition, the emission was enhanced by modifying the energy band of the piezoelectric transistor and reducing the Schottky barrier between the electrode and semiconductor. Furthermore, the ZnO NW arrays regulated the spatial resolution of the device.

2.2. Stretchability

To simulate human skin as much as possible to meet the needs of intelligent systems, the stretchability of tactile sensors is critical. Stretchable conductors and other related electronic components have been extensively studied. A stretchable structure, an intrinsically stretchable conductor, and compounded conductive materials and elastomers are all widely used to implement device stretchability [52,53]. For instance, Guo and co-workers [54] developed a tactile sensor based on an electrode designed with argentum nanofibers (Ag NFs) and silk fibroin. The silk fibroin film exhibited excellent stretchability (>60%). Sun and co-workers [55] developed stretchable e-skin on the basis of precracked Ag nanowires. The resistance linearly varied with the density of cracks over a 30% strain range. Bao and co-workers [15] developed a transistor array based on an intrinsically stretchable polymer, with the design principle of the device illustrated in Fig. 3a. The device could work normally at 100% stretch, either parallel or perpendicular to the direction of current transmission. Since all the major thin films were based on SEBS (i.e., the dielectric, substrate, and 70% CONPHINE semiconductor), interfacial shear and vertical stress were effectively suppressed. In Fig. 3b and c, when a strain of 100% was exerted parallel to the channel direction, the electron mobility merely increased to 0.99 $cm^2/(V\ s)$. Because of its high stretchability, the array could be comfortably attached to objects with naturally irregular surfaces and deformations (such as the palms of people) as a secondary skin, as shown in Fig. 3d. Polymer materials with intrinsically stretchable properties accelerated the development of stretchable tactile sensors [15].

Geometric design of devices is another main approach to achieve stretchability. Cao et al. [56] oxidized a specific part of an elastic substrate to form rigid islands so that the device maintained the shape on the rigid islands under stretched conditions. A stretchable sensor network with an island-bridge structure was constructed that could detect and quantify multiple stimulations to mimic the human somatosensory system. A schematic diagram of the stretchable structure device is shown in Fig. 3e. The sensory nodes of the highly stretchable and conformable matrix network (SCMN) were connected by meandering wires. These meandering interconnects were vital to the implementation of high stretchability and expansibility. A customized pressure test platform was utilized to record the stretching process of the device, as shown in Fig. 3f and g. When the meandering wires were stretched to 800% of the original length, the tension and resistance of the meandering wires did not significantly change. An optical image of the stretched SCMN (scale bar: 2 cm) is shown in Fig. 3h. The sensor could be easily expanded in a specific direction to increase the sensing area [14].

Due to the importance of elastomeric materials and suitable structures for the stretchability of devices, a highly stretchable sensor array that combined Ag NFs with polydimethylsiloxane (PDMS) was developed. As shown in Fig. 3i, by electrospinning, the metal collector was charged to obtain polyvinyl alcohol NFs (PVA NFs) with different orientations, and then, Ag was deposited by magnetron sputtering to metallize the PVA NFs. PDMS acted as a substrate and an encapsulation layer. In this experiment, unidirectional, bidirectional, tridirectional and random Ag NFs were prepared. The effects of the orientation of Ag NFs and the angle of stretch were mainly studied. During the stretching process, although PDMS was used as a substrate to absorb stress through deformation because of its low stiffness, the unidirectional Ag NWs were cracked because of their high effective stiffness, so the device had many cracks at 0°, as shown in Fig. 3j. In Fig. 3k, for the tridirectional Ag NFs, as θ_{max} (the maximum value of the angle between the tensile direction and one of the spinning orientations) increased, the change in resistance decreased. For the multidirectional Ag NF electrode, θ_{max} was always 90°; therefore, this electrode had a better stretchable property, and the resistance only increased 10% after application of 100% strain, as shown in Fig. 3l. Obviously, using multioriented Ag NFs as conductive paths could greatly improve the stretchability of the electrodes [13].

2.3. Self-healing

Human skin can repair itself when exposed to external damage [57]. An ideal tactile sensor should demonstrate a similar capability of repeatable self-healing. A self-healing ability can greatly increase the lifetime of devices when they are damaged. In practical applications, sensors are required to repair damage at room temperature and repair repeated damage at the same location [58]. In recent years, many studies have been conducted on related aspects. The recombination of dynamic molecular bonds can restore the mechanical properties of devices. Self-repairable dynamic molecular bonds mainly include covalent bonds and supramolecular noncovalent bonds [59].

As a typical example, Wang and co-workers [17] introduced dynamic covalent imine bonds as reversible healing sites into a PDMS network. A schematic diagram is shown in Fig. 4a. By the Schiff base reaction, bis(amine)-terminated PDMS and 1,3,5-triformylbenzene generated reversible imine bonds as polymer crosslinker and self-healing points, which were cleaved upon damage and recovered after spontaneous healing. A thin film of a sprayed Ag NW network and a PEDOT film were used as conductors, which were placed on a prestretched PDMS substrate that was then released to produce a periodic wavy structure. Although the Ag-PEDOT film could not heal spontaneously, the healing of the polymer substrate involved fusion of H-PDMS to repair the crack, which exerted a traction force on the Ag-PEDOT film to re-establish electrical contact. The prestretched film had superior flexibility; therefore, the cutting process did not cause damage to the film. When the H-PDMS was completely cut by the blade, its ultimate stress returned to 94% of the initial state after 12 h (21 °C), as shown in Fig. 4b. In addition, Fig. 4c shows that after healing, the initial cleft between the buckled Ag-PEDOT films was clearly restored [17].

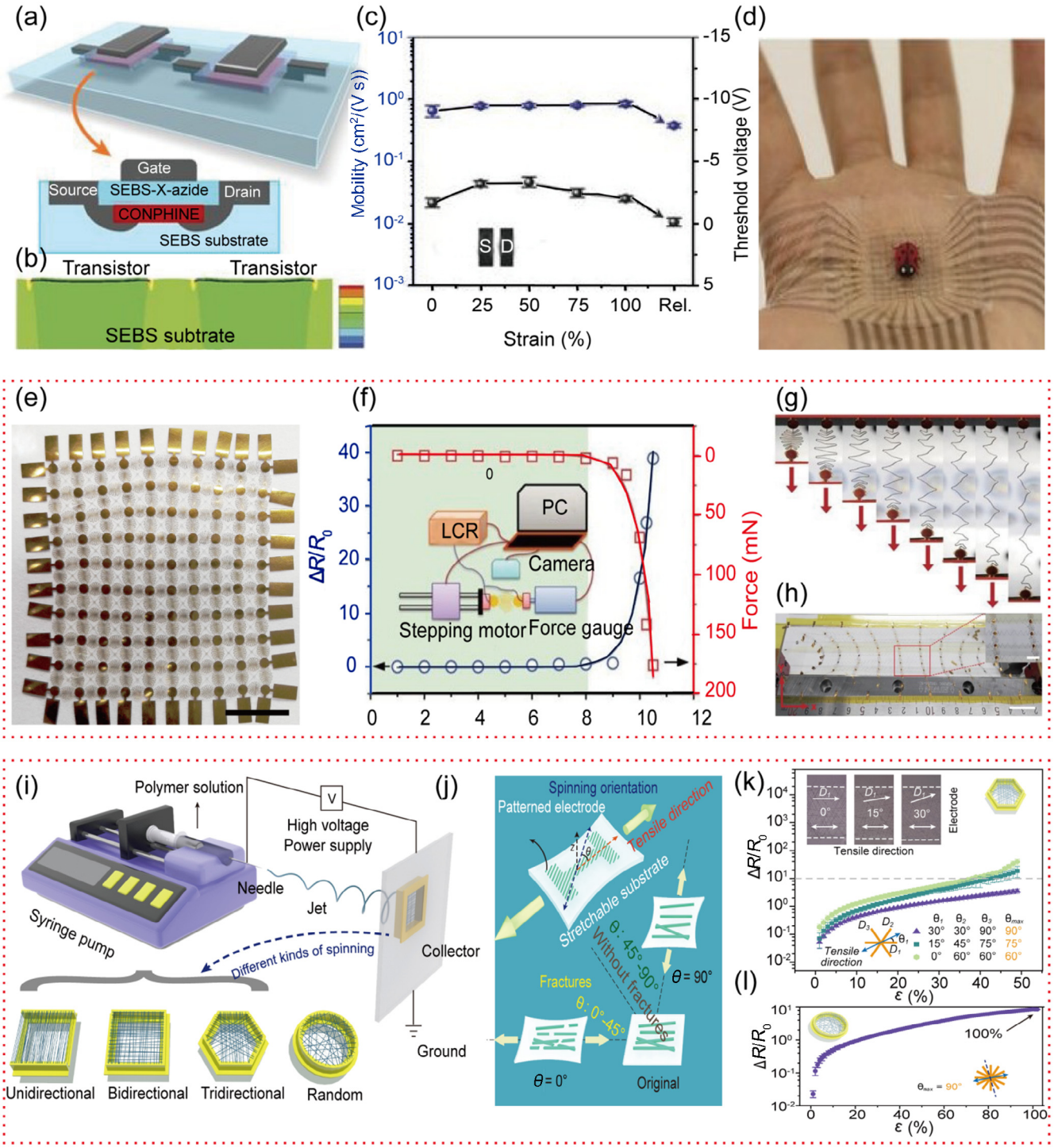

Fig. 3. (Color online) Stretchability of devices. (a) Schematic diagram of an intrinsically stretchable device. (b) Strain distribution in the array when stretched to 100% strain. (c) Mobility and threshold voltage during a parallel stretching cycle. (d) The device was attached to the palm of a hand and was consistent with it. Reprinted with permission from Ref. [15], Copyright © 2018 Springer Nature. (e) Schematic diagram of a stretchable structure device. (f) Relationship between the relative resistance of the device and the change in the force; the green portion is the area where the performance is stable, and the illustration is a schematic of the tensile test platform. (g) Stretchability of meandering wires: L/L_0 from 1 to 8. (h) Extended SCMN (scale: 2 cm); the illustration is an enlarged view of the device after stretching (scale: 5 mm). Reprinted with permission from Ref. [14], Copyright © 2018 Springer Nature. (i) Preparation process of a device in which a stretchable material is combined with a stretchable structure. (j) Deformation of unidirectional Ag NFs at different stretching angles. (k, l) $\Delta R/R_0$ of tridirectional Ag NFs (k) and random Ag NFs (l) varying with tensile strain. Reprinted with permission from Ref. [13], Copyright © 2018 Wiley-VCH.

In addition to covalent adaptive bonds, supramolecular noncovalent bonds are another type of bond that can achieve self-healing. These bonds are involved in hydrogen bonding, metal–ligand coordination, π-π stacking, host–guest complexation, etc. [60–63]. Bao and co-workers [16] developed a sensor that can repair itself at room temperature. The self-healing mechanism mainly occurred through the reaction of oligomeric chains and μNi particles. As shown in Fig. 4d, a randomly branched network

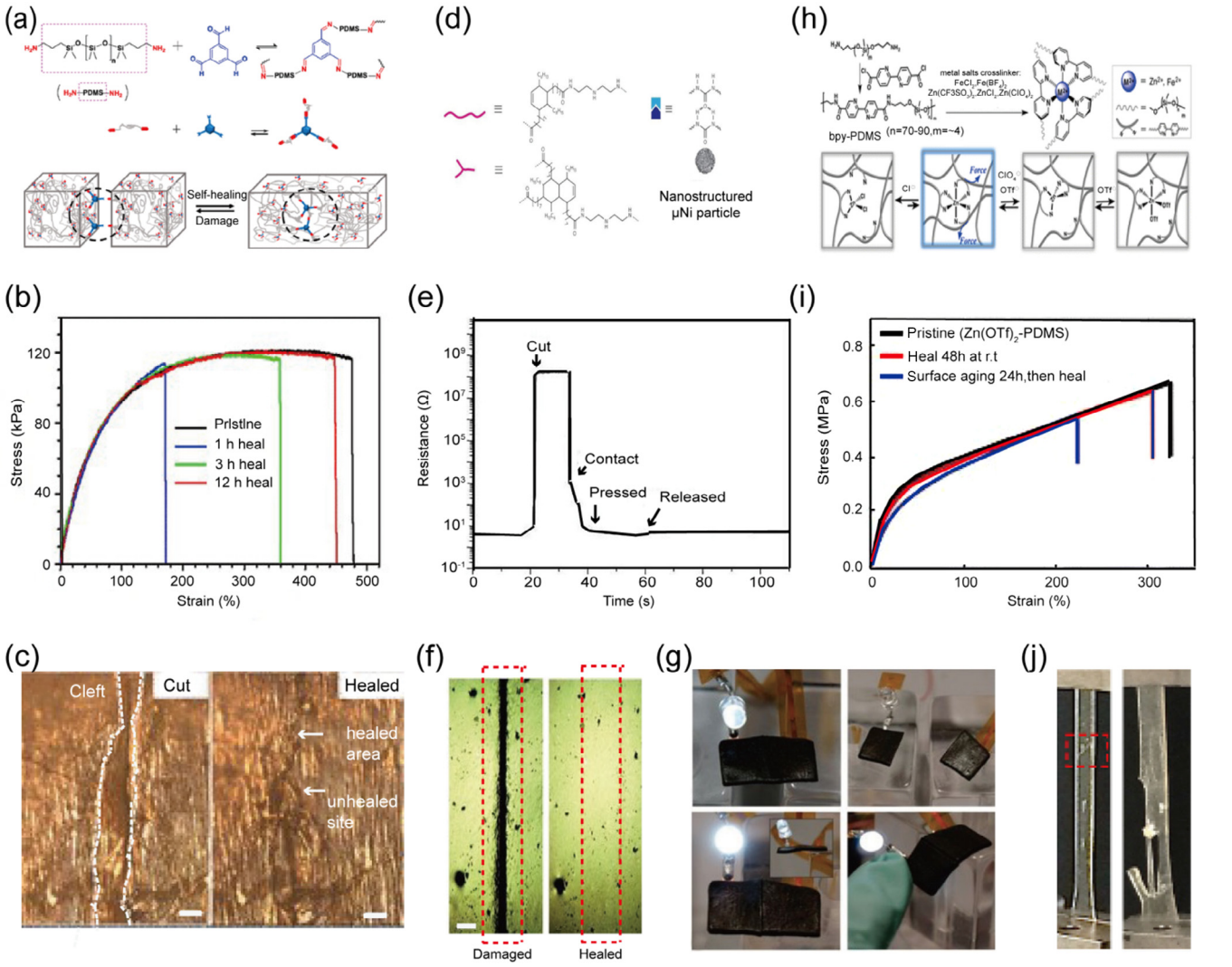

Fig. 4. (Color online) Self-healing of devices. (a) Self-healing was achieved by dynamic covalent imine bonds. Bis(amine)-terminated PDMS and 1,3,5-trimethylbenzene formed a reversible imine bond by the Schiff base reaction, which cleaved after injury and recovered during autonomous healing. (b) After being cut by a razor blade, the H-PDMS healed at different times under ambient conditions (21 °C). (c) Microscopic image of a new cut and the healing H-PDMS/Ag-PEDOT membrane at 12 h. Scale bar: 100 μm. Reprinted with permission from Ref. [17], Copyright © 2018 American Chemical Society. (d) Self-healing mechanism of supramolecular bonds (hydrogen bonds). The linear and branched polymers formed a random branching network, and the urea groups at the ends of the branched polymer formed the primary hydrogen bonds between the polymer chains. (e) During the healing process of the device, the resistance basically returned to the original value after 60 s. (f) Optical microscopy images of damaged samples and complete scar healing samples. Scale bar: 1 mm. (g) After self-healing of the conductive composite material, the LED was illuminated again. Reprinted with permission from Ref. [16], Copyright © 2012 Springer Nature. (h) Self-healing mechanism of supramolecular bonds (metal–ligand coordination bonds). Dynamic interaction between the metal cation Zn^{2+}, ligand and counter anion in the polymer system under mechanical stress. (i) Self-healing of the $Zn(OTf)_2$-PDMS polymer under ambient conditions. (j) Schematic diagram of the device after being cut and broken into two parts and subsequent self-healing. The broken part completely healed itself. Reprinted with permission from Ref. [59], Copyright © 2016 American Chemical Society.

was formed by linear and branched polymers, and hydrogen bonds were formed by urea groups at both ends of the branched polymer. The self-healing property of the supramolecular polymers was based on many weak hydrogen bonds, which were preferentially broken under mechanical damage. Through the dynamic association and dissociation of these "broken" hydrogen bonds at room temperature, the fracture surface underwent a passive healing process. In addition, the low glass transition temperature caused the polymer chains to rearrange, wet and diffuse at the fracture interface, which allowed completion of the self-healing process at ambient temperatures. Fig. 4e and f show the electrical healing process over time. When a light pressure was applied onto the wound for 15 s, the conductivity of the polymer was close to the initial value. After cutting and the self-healing process at the same position three times, the conductivity still recovered well. Fig. 4g shows the connection between the electrical conductor and LED. The accomplishment of the self-healing process of the electrical conductor was shown by the lighting of the LED [16].

Additionally, dual-strength dynamic metal-ligand coordination bonds, which can create attractive interactions, were embedded into PDMS to obtain the self-healing property. Fig. 4h shows the self-healing process of supramolecular bonds. The attractive metal-ligand coordination interactions as a broad molecular parameter can be used to impart desirable material properties by changing the metal ions, counterions, and ligands to adjust the bond strength. The bipyridine moiety has good coordination geometry with many transition metal ions, which can be used to direct self-assembly of polypeptides and construct metal–organic frameworks (MOFs) or molecular knots. Metal salts can be additional knobs for adjusting the crosslink density and polymer kinetics [64]. To test the self-healing performance, the relationship of strain and stress between the original membrane and the self-healing Zn

$(OTf)_2$-PDMS membrane is shown in Fig. 4i. The healing efficiency reached 76%±22%. In addition, the surface aging effect had no effect on the self-healing efficiency. The broken surface of the $Zn(OTf)_2$-PDMS film maintained a self-healing efficiency of ~60% after exposure to the environment for 24 h. Fig. 4j shows the $Zn(OTf)_2$-PDMS film with the self-healing capability, and the dotted box marks the joining of the edges after healing. To verify the feasibility of using metal ion crosslinked PDMS as a gate insulator, organic field-effect transistors (OFETs) were fabricated using the bottom-contact top-gate device of a p-type or n-type polymer semiconductor, and metal salt crosslinked PDMS was integrated into this device as a dielectric layer. The dielectric constant of crosslinked PDMS with $FeCl_2$ or $ZnCl_2$ was increased in comparison to PDMS, and the transistors showed hysteresis-free transfer performance [59].

2.4. Self-powered capability

Devices powered by ordinary batteries need to be repeatedly recharged, which involves a great consumption of nonrenewable energy. At the same time, a battery has a limited service life so will cause certain damage to the environment [65]. In addition, the large size, weight and hardness of batteries also restrain their application in micro-nano flexible electronic devices for intelligent systems. Therefore, collecting energy from nature and converting it into electrical energy have great significance for tactile sensors in the future [66]. Research on the collection of energy from nature has mainly focused on four aspects. First, solar cells were designed based on the photovoltaic effect to collect solar energy. Second, the thermoelectric effect was introduced to convert collected thermal energy into electricity. Third, piezoelectric nanogenerators (PENGs) were designed based on the piezoelectric effect. Finally, triboelectric nanogenerators (TENGs) were developed based on the triboelectric effect, which both convert mechanical energy into electricity [67–70].

The first PENG was demonstrated by Wang and Song [71] in 2006, which was fabricated with ZnO nanowires. In recent years, various tactile sensors based on the piezoelectric effect have been rapidly developed. Shi et al. [72] developed a PENG based on cellulose/$BaTiO_3$ and PDMS nanocomposites. The maximum voltage was 15.5 V, with a corresponding maximum power of 11.8 μW. Ryou and co-workers [73] fabricated a piezoelectric generator based on flexible materials with a group III nitride (III-N) thin film. Its open-circuit voltage was 50 V, and the maximum power was 167 μW. Subsequently, in 2012, a TENG was first mentioned by Wang group, providing a new idea for harvesting small-scale mechanical energy from daily life [74]. The principle of a TENG is based on the coupling of triboelectrification and electrostatic induction. A TENG has the following four basic working modes: the single-electrode mode, vertical contact-separation mode, lateral sliding mode, and freestanding triboelectric layer mode [75]. Among them, an external pressure is perpendicularly applied onto the contact surface for the single-electrode mode and vertical contact-separation mode; therefore, the two modes are more suitable for designing tactile sensors. Briefly, the principle of the vertical contact-separation mode is that two dielectric films are in contact with each other, forming opposite charges on the contact surface. When an external force separates the dielectric films, the two electrodes form an induced potential difference [76]. Jeon et al. [77] developed a TENG based on the vertical contact-separation mode, which was prepared by forming a ZnO nanostructure layer on an ITO-coated polyethylene naphthalate two formic acid glycol ester (PEN) substrate. The output voltage of the TENG was approximately 20 V. Dudem and co-workers [36] used polyaniline (PANI)-coated cotton textile to design a TENG, which could be configured in the vertical contact-separation mode or single-electrode mode. When this TENG was in the vertical contact-separation mode, the highest output voltage and power density were approximately 350 V and 11.25 W/m^2. Cheedarala et al. [78] developed a TENG with a modified woven carbon fiber mat and a PVDF membrane as two friction layers. To realize contact and separation, a spring structure was designed. Owing to the interaction of the two friction layers, the authors obtained a high output voltage of 95 V and a short-circuit current of 180 μA.

The vertical contact-separation mode requires two electrodes connected by a load. However, in our daily life, some parts of a TENG involve movement, for example, the energy generated by the friction between a human walking and the earth; thus, connection by wires to electrodes is not feasible. To more conveniently collect mechanical energy in this case, a TENG with the single-electrode mode was proposed. Contact and separation occur between the upper charged object and the lower object, thus changing the distribution of the local electric field. To balance the potential, the electrode and ground exchange electrons with each other [79]. Zhao et al. [80] used carbonized polyacrylonitrile nanofiber films (PAN NFs) as electrodes, embedded barium titanate nanoparticles (BTO NPs) into the NFs to produce the piezoelectric effect and then used PDMS as the encapsulation layer and triboelectric layer, as shown in Fig. 5a. SEM image of carbonized PAN/BTO NFs is shown in Fig. 5b. Based on the single-electrode mode, when a hand touched the PDMS, its surface was electrified due to friction. Meanwhile, the contact stress caused the BTO to deform, which resulted in the generation of a local piezoelectric potential that enhanced the potential of the surface. When the hand was removed, an equal amount of positive charge was generated on the PAN-C/BTO NF layer because of electrostatic induction, accompanied by the flow of charge, as illustrated in Fig. 5c. The open-circuit voltage and short-circuit current of the device were tested under different external pressures, as displayed in Fig. 5d. The electrical output (R_V^2 = 0.996 for V_{oc} or R_I^2 = 0.994 for I_{sc}) and pressure had a good linear relationship from 0.15 to 25 N, which indicates that this type of device is reliable in pressure detection. A TENG based on the single-electrode mode was proposed by Fang et al. [81], with the fundamental structure exhibited in Fig. 5e. The device had a structure of PDMS-supported Ag nanowires, which could be used in intelligent systems and artificial skin. The contact-separation between PDMS and a finger was used to convert the friction signal into an electrical signal. The single-electrode TENG had a high electrical output. Fig. 5f, g shows that the peak value of the open-circuit voltage was approximately 70 V, and the short-circuit current density reached 1.5 mA/m^2 [81].

2.5. Biodegradability

With the increasing demand for intelligent devices, devices with novel performance must be developed to solve the problem of electronic waste. Therefore, the study of transient electronics has great significance. Furthermore, in the medical field, sensors have been widely used as medical devices to monitor health or treat some diseases, such as arrhythmia and bradycardia [82]. For the treatment of diseases, usually, the devices must work for a period of time. Therefore, when devices are implanted *in vivo*, biodegradability is extremely important. Good biodegradability can avoid secondary surgery for patients, which makes the treatment of diseases safer, simpler and more reliable [83].

To reach these goals, inorganic materials were first applied. In particular, silicon-based electronic devices play representative roles because of their ability to hydrolyze under physiological conditions. Biodegradable tactile sensors can be composed of silicon nanofilms and inorganic films, such as magnesium or magnesium oxide [20]. For example, Hwang and co-workers [84] developed a silicon-based strategy to fully form transient circuit components and circuits, relying on a combination of a particular type of silicon

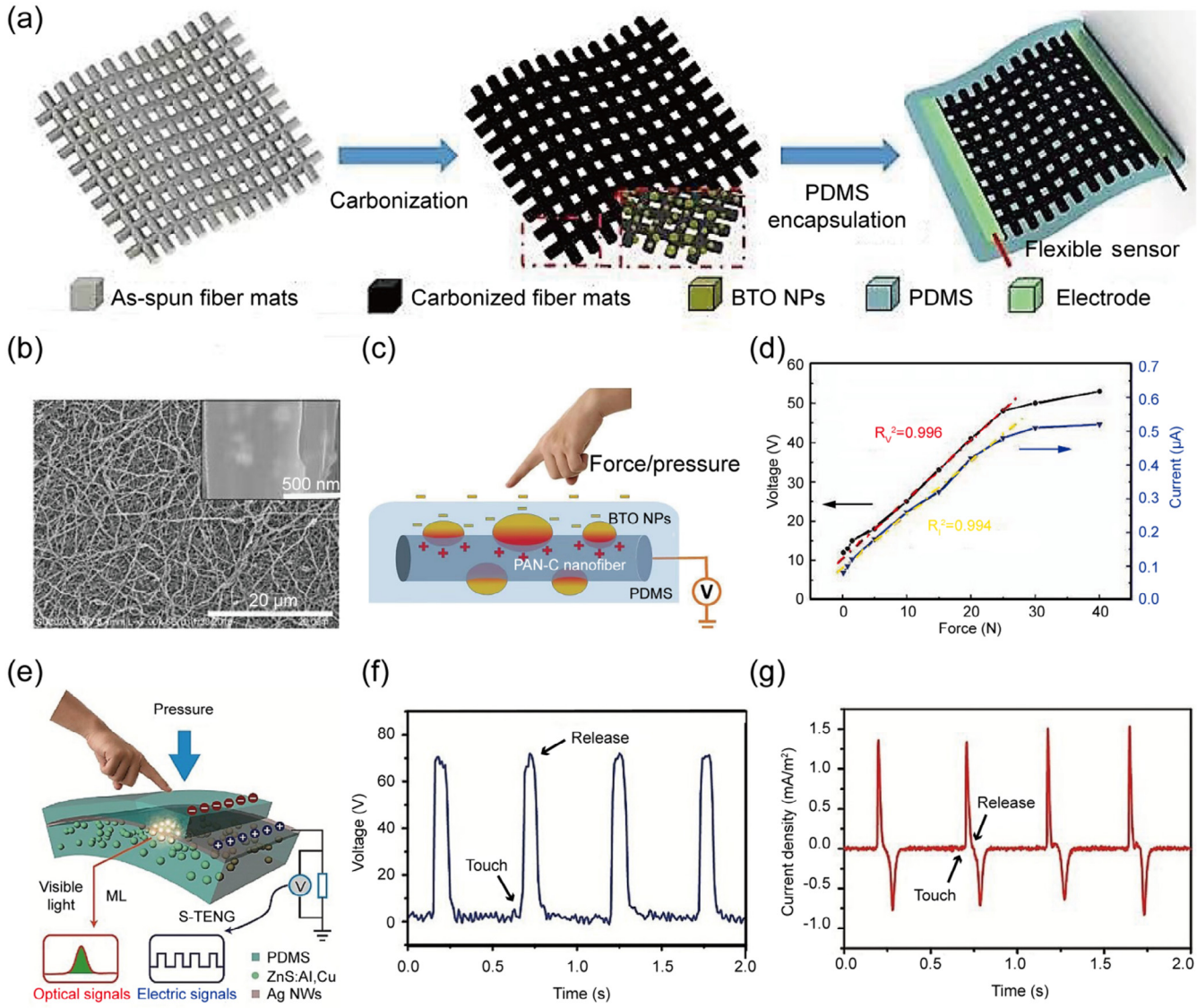

Fig. 5. (Color online) Self-powered performance of devices. (a) Schematic diagram of the preparation process of a self-powered sensor based on a carbonized PAN/BTO NF. (b) SEM image of carbonized PAN/BTO NFs. (c) Schematic diagram of the self-powered sensor combined with the piezoelectric effect and triboelectric effect. (d) Open-circuit voltage and short-circuit current of the device under different pressures. Reprinted with permission from Ref. [80], Copyright © 2018 American Chemical Society. (e) Schematic diagram of a self-powered sensor based on the single-electrode mode. Output voltage (f) and current density (g) during periodic contact-separation between fingers and devices. Reprinted with permission from Ref. [81], Copyright © 2016 Wiley-VCH.

on insulator (SOI) wafer and transfer printing technology. The materials of the device were all water-soluble, including silicon, siloxane, magnesium, magnesium and silk. And their applications in the manufacture of various electronic components and simple logic gates were demonstrated and their transient characteristics were studied. Canan et al. [85] put forward the concrete design and manufacturing plan of ZnO thin film optical transistor and mechanical energy harvesters (also can be used as a strain gauge) and introduced several electronic devices based on ZnO. The key features of these could be completely dissolved in the water or biofluids. Meanwhile, the kinetics of dissolution and the ability to control dissolution using materials and design choices are studied in detail. However, tactile sensors based on inorganic materials are rigid and require high technology and high cost. Later, to increase the flexibility of tactile sensors, miniaturize them and reduce the manufacturing cost, breakthroughs were made in the field of organic materials. The preparation process of organic electronics is more environmentally friendly. Some biodegradable small molecules have been reported, such as indigo derivatives and β-carotene [21,86,87]. Wang and Li groups [88] developed a biodegradable TENG (BN-TENG) based on natural materials to treat heart disease. The structure of the device is shown in Fig. 6a. In this experiment, all biodegradable materials came from nature, including cellulose, rice paper, silk fibroin, egg white and chitin. The BN-TENG included polymers (NBPs) and Mg electrodes. Any two different NBPs could be made from the five natural materials mentioned above for use as the triboelectric layer, and an ultrathin Mg film was used as the back electrode. The surface of the triboelectric layer was treated by inductively coupled plasma (ICP) to form an array of nanostructures to improve the effective contact area and contact electrification. The biodegradability performance was characterized *in vitro* and *in vivo*. Fig. 6b (top) shows the biodegradation process *in vitro*. BN-TENGs encapsulated with silk fibroin were placed in phosphate buffer solution (PBS). The structure was intact on the first day. Over time, the skeleton of the polymer was broken, autocatalytic hydrolysis occurred, and finally, the

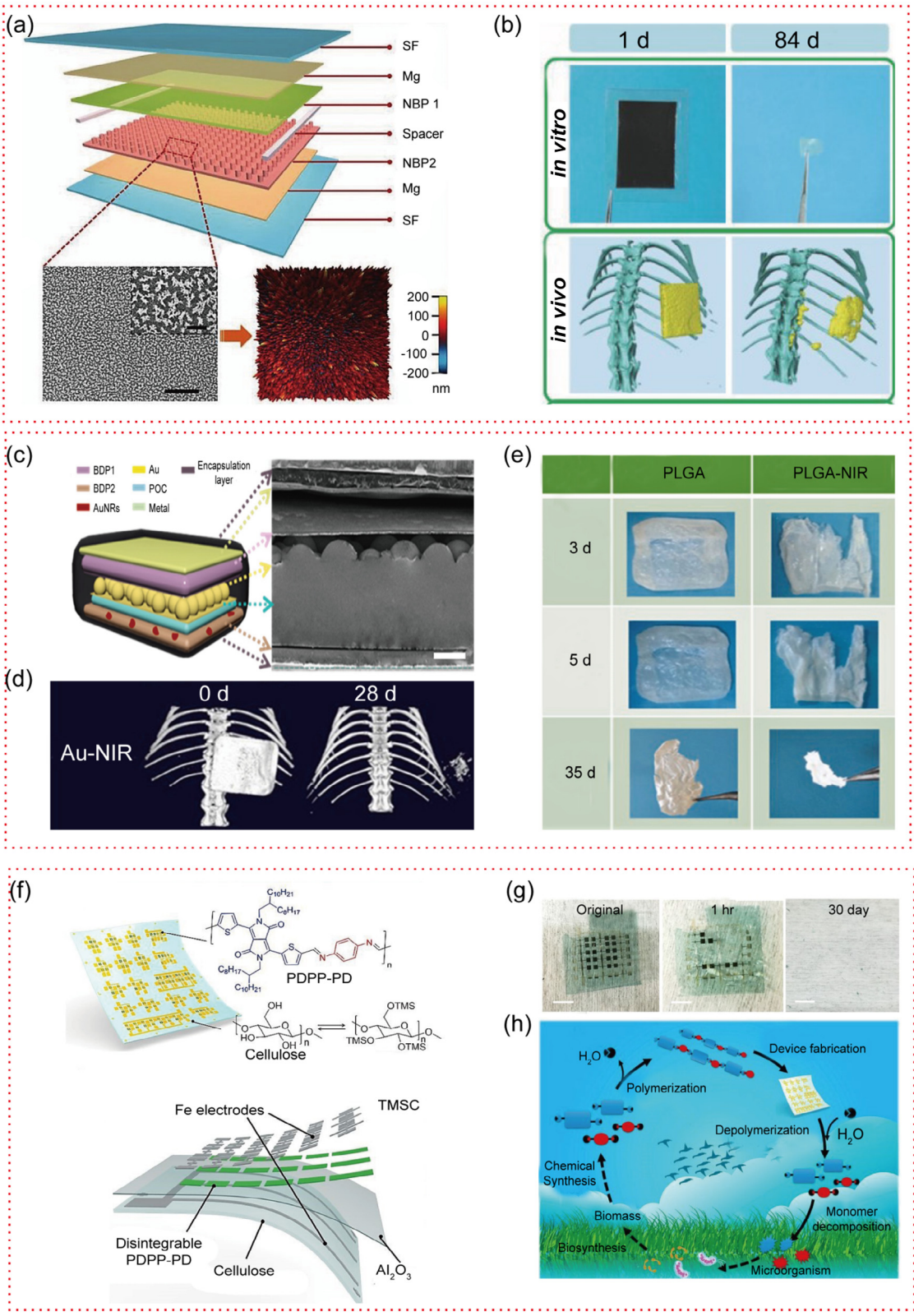

Fig. 6. (Color online) (a) Schematic diagram of a BN-TENG based on biodegradable organic polymers derived from nature. Lower and upper scale bars: 5 and 1 μm. (b) Degree of degradation of the device after different times *in vitro* (top) and *in vivo* (bottom). Reprinted with permission from Ref. [88], Copyright © 2018 Wiley-VCH. (c) Schematic diagram of a device prepared from a synthetic biodegradable organic polymer. Scale bar: 500 μm. (d) Degradation process of the device *in vivo*. (e) Degradation process of the device *in vitro*. Reprinted with permission from Ref. [89], Copyright © 2018 Elsevier. (f) Schematic diagram of a biodegradable material and structural diagram of the device using a reversible imine bond. (g) Process of device degradation. (h) Ideal cycle diagram for the synthesis, fabrication, and decomposition of transient polymer electronics. Reprinted with permission from Ref. [23], Copyright © 2017 National Academy of Sciences.

whole structure was dissolved in PBS. As shown in Fig. 6b (bottom), BN-TENGs encapsulated with silk fibroin were placed in SD rats. The biodegradation process was roughly the same as that *in vitro*, and the cracked parts were degraded and absorbed by the SD rat. However, the biodegradation process could not be controlled from the outside. To achieve regulation of the biodegradation process, a tunable biodegradable implantable TENG (BD-iTENG) was fabricated by Wang and co-workers [89], and the biodegradation process was studied *in vivo* and *in vitro*. Fig. 6c shows that the ability of the BD-iTENG to respond to near-infrared (NIR) irradiation derived from the polylactic acid-glycolic acid copolymer (PLGA) membrane doped with gold (Au) nanorods in the BD-iTENG, so we could use some external conditions to control the biodegradation process. The BD-iTENG included three parts: (1) an array of hemispherical structures was deposited with Au as both a triboelectric layer and a bottom electrode; (2) a biodegradable polymer layer was deposited as another triboelectric layer, on which Mg was deposited as an upper electrode; and (3) another biodegradable polymer layer doped with Au nanorods acted as a substrate. Fig. 6e shows that the BD-iTENG was placed in PBS at 37 °C for 35 d. In the absence of NIR treatment, a majority of the PLGA-iTENG was hydrolytically degraded by PBS after 35 days. When the BD-iTENG device was treated by NIR, the degradation rate was significantly increased. After that, PLGA-iTENGs treated by NIR were implanted into the body of SD rats. Fig. 6d shows that the PLGA-iTENGs gradually degraded into fragments within 28 d. After one NIR treatment, the voltage decreased to 0 at the 24th hour.

In addition to some natural materials and the synthetic materials mentioned above that have biodegradability, conjugated polymers have been developed to achieve biodegradability of tactile sensors for intelligent systems. Conjugated polymers are considered candidates for field-effect transistors (FETs) due to their good flexibility, simple preparation techniques, and high carrier mobilities [90]. Bao's group [23] demonstrated a thin-film transistor with a semiconductor polymer, which was composed of reversible imine bonds and provided building blocks. In addition, this transistor easily decomposed under mild acidic conditions. Fig. 6h shows several key processes of the "ideal cycle". The synthesis of semiconducting polymers from substances in nature and their eventual decomposition in the environment are anticipated. In the study by Bao et al., the imine bond was used as a "reversible conjugated linker", as illustrated in Fig. 6f. To realize biodegradability of the whole electronic device, iron (Fe) was introduced as a gate electrode, and a source-drain electrode of the polymer and PDPP-PD was synthesized via the condensation reaction. The degradation process of the flexible device is shown in Fig. 6g. The Fe electrode quickly degraded within 1 h under certain conditions, and the conjugated polymer, cellulose substrate and alumina could be fully degraded within 30 d. In practical applications, the use of suitable decomposable encapsulation materials could potentially enable control of the rate of device degradation.

3. Applications in intelligent systems

Due to the high performance of tactile sensors, they are being applied to intelligent systems increasingly frequently. In this section, we introduce three application areas and the latest researches in intelligent systems. Wearable devices offer broad prospects for the development of mobile medical and visualization devices [91]. In the field of biomedicine, special function devices provide ideas for the design of disease monitoring systems *in vivo* and *in vitro*, as well as antibacterial platforms. The development of electronic signature systems makes data collection and management more convenient and guarantees the security of personal information [92]. The study of electronic skin not only enables the realization of more intelligent robots but also has important significance in medical treatment.

3.1. Wearable devices

The materials used to fabricate wearable devices must meet the requirements of being flexible, lightweight, breathable and biocompatible and having some special function. Wearable devices not only provide an approach to real-time health monitoring and personal communication but also have convenient portability [93]. Consequently, significant efforts are being made to develop wearable devices.

Primarily, wearable devices are applied in real-time health monitoring. Li and co-workers [94] developed a flexible nanogenerator (NG) that acted as a wearable self-powered breathing sensor for real-time monitoring of human breathing. The poly(vinylidene fluoride) (PVDF) film prepared by electrospinning acted as a piezoelectric layer due to its high piezoelectric voltage constant. Au was deposited as the top and bottom electrodes on the two sides of the PVDF film. The piezoelectric NG was placed on the chest of a man. Using the platform of the piezoelectric active sensor based on the PVDF piezoelectric film (PEAS) and a Biopac MP150 physiological signal recording system, different frequency respiratory signals were measured. The PEAS and Biopac MP150 were highly consistent at different respiratory rates, and these breathing curves contained detailed information about the dynamics of the respiratory process. The PEAS was used to detect vibration of the vocal cords. No signal was observed when no sound was heard. When 'P, I, E, Z, O' were spoken, regular high frequency signals appeared. Different letters had different piezoelectric signals. Therefore, the PEAS for use in quantitative diagnostic techniques might evolve as a wearable and zero-power-consumption device in the future.

Smart textiles can change depending on the environment, such as temperature and color. A communicative textile with a large area can be made and easily integrated into a human. Among smart textiles, light-emitting textiles have aroused great interest because of their high visibility, security and fashionability [95]. One of the most typical light-emitting textiles is realized by weaving optical fibers according to a specific pattern and incorporating them into the textile. Jeong and co-workers [96] designed a mechanoluminescent (ML) textile that used the movement of a human as the power source to drive the optical fibers to emit light. Stretching of a muscle could cause mechanical deformation of the fibers. As shown in Fig. 7a, ZnS particles were doped with metal ions and embedded in PDMS + ZnS, and a cross-shaped fiber frame was used to make the contact area with PDMS + ZnS larger, which improved the adhesion between the materials. At the same time, the use of an organofunctional silane coupling-based primer improved the reactivity and adhesion of the fibers. After that, the fiber coated by PDMS + ZnS was covered with Si(adh) to fill the gaps or defects in PDMS + ZnS. The PDMS + ZnS was surrounded and 3D localized by three contact points. The authors used a shuttle to tightly bind the fabrics together. The Si(adh) was transparent, so the edges of the fibers indicated that Si(adh) adhered well to the fibers and PDMS + ZnS. Fig. 7b shows a photograph of the weaving process of ML fibers. To verify the ML properties, we applied tension to the ML fabric and observed green light, as shown in Fig. 7c.

In addition to ML fibers, electroluminescent fibers can also be integrated into fabrics for the preparation of multifunctional wearable electronic devices [98]. A novel electroluminescent textile display obtained by a continuous one-step extrusion process was demonstrated by Zhang and co-workers [97], as shown in Fig. 7d. A combination of ZnS powder and a silicone elastomer formed the electroluminescent material. The silicone elastomer acted as both a protecting layer and a dielectric layer. The design of the

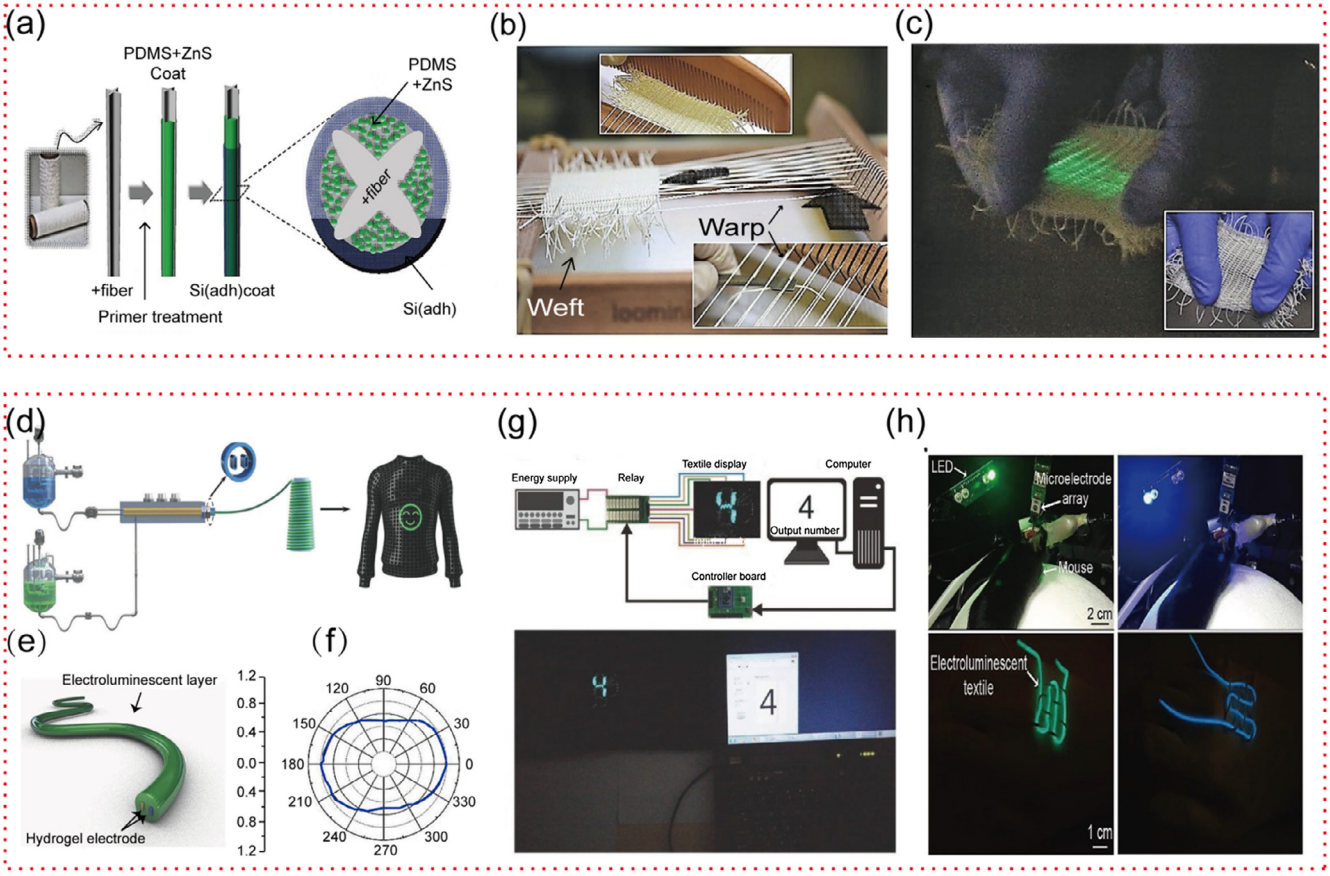

Fig. 7. (Color online) Application of sensors in intelligent wearable devices. (a) Schematic diagram of the preparation process of textiles based on mechanoluminescence. (b) Photograph of the weaving process of ML fibers. (c) The fiber emitted light when it was stretched. Reprinted with permission from Ref. [96], Copyright © 2017 Wiley-VCH. (d) Schematic diagram of the preparation process of an electroluminescent textile. (e) Two internal electrodes were covered by an electroluminescent layer. (f) The device had different brightness values at different angles. The maximum brightness appeared at 0° and 180°. (g) The display of the device could be controlled by a computer. (h) The illumination color of the device could be controlled by the brain. Top: the neural activity of mice was recorded. Bottom: the display color of the textile was consistent with the color of the given light source. Reprinted with permission from Ref. [97], Copyright © 2018 Wiley-VCH.

two elliptical hydrogel electrodes increased their face-to-face area so that they could emit stronger light, as shown in Fig. 7e. PVA and poly(ethylene oxide) (PEO) were used as internal conducting electrodes. Due to the unique fiber structure, the super-stretchable electroluminescent fibers (SEFs) could emit light in all directions, but the maximum luminance was at angles of 0° and 180°, as shown in Fig. 7f. When the length of the SEFs reached the meter level, the change of luminance along the axial direction was less than 5%. Although green light was dominant, other colors, such as yellow and blue, could also be achieved by selecting the desired ZnS powder. The SEFs could be stretched to 800%. Moreover, the fibers also had extremely high stretchability and could be stretched up to 800%. As shown in Fig. 7g, the textiles could be connected to a computer. When different numbers were entered into the computer, different numbers were displayed on the textile. Afterwards, using the integrated platform, a brain-interfaced camouflage system was constructed, in which the color of the electroluminescent textile could be determined by the decoded neuron, and when the ambient light changed from green to blue, the textile could quickly respond with discoloration, as shown in Fig. 7h.

3.2. Biomedical field

Biomedical tactile sensors are mainly composed of two key parts: the part for receiving and generating the signal of tactile sensors and the hardware instruments of the devices for converting the physical signal. The former mainly include electrical and optical detection components, such as current/potential measuring electrodes, piezoelectric crystals and FETs [99–101]. The emergence of various new materials and new technologies has enabled biomedical tactile sensors to be miniaturized, multifunctionalized, integrated and made intelligent. At present, thermosensitive biomedical sensors, FET biomedical sensors, piezoelectric biomedical sensors, triboelectric biomedical sensors and photosensitive biosensors have been widely used in biomedical research [102].

Among them, triboelectric biomedical tactile sensors have gained great attention because of their self-powered capability, low power consumption and high sensitivity. A self-powered ultrasensitive pulse sensor (SUPS) for intelligent mobile diagnosis of cardiovascular disease was developed by Wang and co-workers [103]. The design principle of the device was the coupling effect of contact electrification and electrostatic induction. A schematic diagram of the device is shown in Fig. 8a. A Kapton thin film and an ultrathin copper (Cu) layer with nanostructures were used as two triboelectric layers. The ultrathin Cu layer and another Cu layer plated on the back of the Kapton film were used as electrodes, and PDMS was used as an encapsulation layer. The device adopted concave structures to ensure an excellent correspondence between the force and the electrical signal. Heart rate variability (HRV) is a convincing predictor of cardiovascular disease, and the geometry of the HRV Poincare plot was used to clinically distinguish the health of subjects. Fig. 8b, c show the Poincare plots constructed

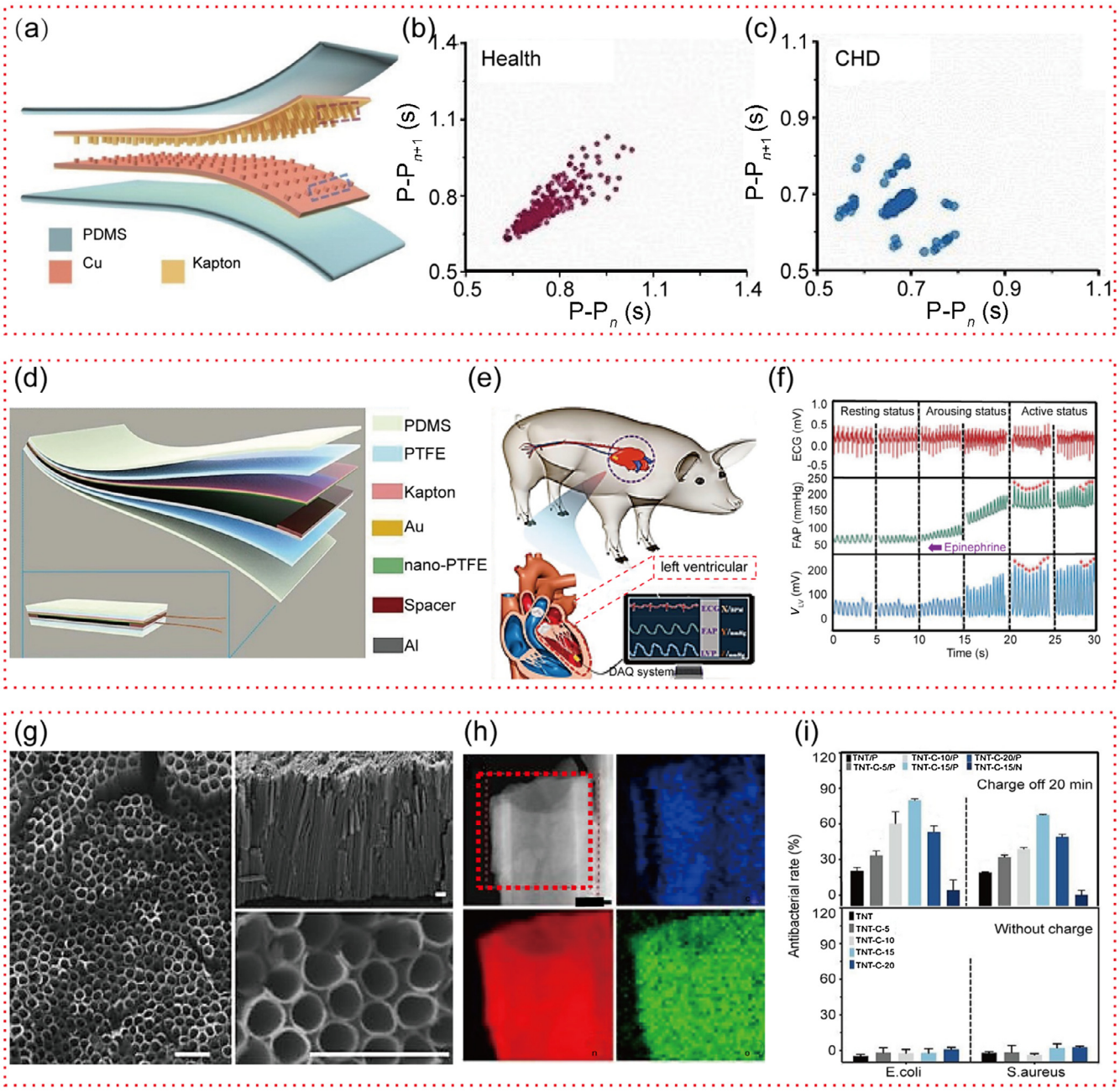

Fig. 8. (Color online) Application of tactile sensors in intelligent biomedicine. (a) Schematic diagram of a pulse sensor for *in vitro* disease diagnosis. Poincare plot of healthy people (b) and people with CHD (c). Reprinted with permission from Ref. [103], Copyright © 2017 Wiley-VCH. (d) Schematic diagram of an endocardial pressure sensor for *in vivo* disease diagnosis. (e) The device was implanted into an adult Yorkshire swine's heart to acquire signals. (f) Comparison of ECG, FAP, and SEPS working signals under different physiological conditions. Reprinted with permission from Ref. [104], Copyright © 2018 Wiley-VCH. (g) SEM image of capacitance-based antibacterial platform TNT-C-15. Scale bar: 500 nm. (h) STEM and EELS images of the device. C was evenly distributed throughout the tube wall. (i) Antibacterial effect under different conditions. Reprinted with permission from Ref. [105], Copyright © 2018 Springer Nature.

from the radial artery pulse of a healthy person and a patient with coronary heart disease (CHD). The Poincare plot of a healthy person was comet shaped or elliptical; however, a Poincare plot with shorter width and length indicated that the patient had CHD, proving that the SUPS was effective in the diagnosis of cardiovascular disease. The system is expected to find application in intelligent mobile diagnostic systems.

To prepare biomedical devices that could be implanted into the body, Wang and Li made some efforts in this field. For patients with impaired cardiac function, the changes in endocardial pressure have a certain determinant role [106]. Based on a TENG, a flexible, miniaturized, self-powered endocardial pressure sensor (SEPS) was fabricated, which was minimally invasively implanted with surgical catheters. As shown in Fig. 8d, polytetrafluoroethylene (PTFE) etched by ICP was used as a triboelectric layer, an aluminum (Al) foil was used as another triboelectric layer, and a 3D ethylene–vinyl acetate (EVA) copolymer film acted as a barrier to ensure contact-separation between both triboelectric layers. The nano-PTFE surface was modified by corona discharge to achieve a high surface charge density and improve the sensitivity and output performance of the SEPS. To simulate the role of the SEPS in biomedical real-time monitoring, the authors chose male

adult Yorkshire pigs (40 kg) as the animal model, as shown in Fig. 8e. They combined the miniature SEPS with a polyvinylchloride (PVC) retractable catheter to construct a delivery system to achieve minimally invasive implantation. The working signals of electrocardiography (ECG), the femoral arterial pressure (FAP), and the SEPS were compared in the resting, waking, and active states, as shown in Fig. 8f. In the resting state, the device had little effect on the stability of the cardiac functionality. In the active state, the SEPS responded to endocardial pressure, and the peaks of the SEPS outputs showed slight fluctuations with the systolic FAP (arrows), indicating that the endocardial pressure remained high. Furthermore, the device still had a high sensitivity to small changes [104].

In many clinical applications, antibacterial properties are also of great significance. Physiologically, electrical interactions cause changes in bacterial morphology. Therefore, Chu and Li group [105] were inspired to design light-independent antibacterial materials and introduced other sterilization measures, such as using electrically modified biological materials to supplement light irradiation. Titanium metal foil was placed in NH_4F-ethylene glycol solution for electrochemical anodization to prepare titania nanotubes, and then, the obtained carbon nanotubes were annealed in argon (Ar) to prepare ordered carbon-doped capacitive titanium dioxide nanotubes (TNT-C), as shown in Fig. 8g. Scanning transmission electron microscopy (STEM) and electron energy loss spectroscopy (EELS) demonstrated that Carbonium (C) was evenly distributed across the entire tube wall, as shown in Fig. 8h. An impressed current was applied to the TNT-C to evaluate the bactericidal ability. In different TNT-C samples, TNT-C-15 with the highest capacitance had the highest inhibition rate, which indicated that the antibacterial property of the TNT-C sample was related to the capacitance and the thickness of the bacterial membrane after charging, as shown in Fig. 8i.

3.3. Man-machine interaction and intelligent robots

Practical breakthroughs in advanced tactile sensor technologies, such as image recognition, voice recognition, pressure recognition and temperature recognition technologies, have led to significant improvements in man–machine interaction and the perceptual capabilities of robots [107]. Electronic devices and robots are beginning to enter a new era of intelligence.

Among them, the man–machine interaction system realizes the transformation of information into a human acceptable form. A wafer-scale flexible pressure sensor was invented that achieved secure signature collection by recording the signer's handwritten pattern and signing habits. The device used ML materials (ZnS:Mn particles), which were bonded with polyethylene terephthalate (PET) to form a sandwich structure, as shown in Fig. 9a. In the single-point dynamic pressure recording and two-dimensional planar pressure mapping mode, the devices responded immediately to the stimulation through the mechanoluminescence process, which converted the pressure signal into an optical signal. Fig. 9b shows the image acquisition process and the information processing system. As shown in Fig. 9c, by pressing a stamp onto the pressure sensor matrix (PSM) device, a "rose-shaped" pressure profile on a two-dimensional plane was obtained. Fig. 9d shows the recorded results of the signing habits of several signers. Through the signer's handwritten "piezo" and the corresponding ML intensity distribution, differences in morphology could be clearly observed. According to the image, we could also see personal handwriting habits, such as the pressure on each pixel and the handwriting speed [108]. In addition, the choice of different materials allowed the device to emit light of different colors. Piezoelectric material CaZnOS:Er^{3+} particles exhibit mechanoluminescence and upconversion luminescence properties. The device was a flexible film made of two polyethylene terephthalate substrates with CaZnOS:Er^{3+} particles coated between them, and green light could be observed [110]. Lanthanide-ion-doped CaZnOS:Sm^{3+} emitted red light upon stimulation by a dynamic mechanical stress [111].

Through the coupling effect of photoluminescence and triboelectrification, a stretchable intelligent skin for tactile perception and gesture sensing as developed. Fig. 9e shows a schematic diagram of the tactile sensor. A flexible tightly bonded microcracked metal film with an aggregation-induced emission (AIE) compound served as an active substrate. The microcracks acted as "gates" to regulate the exposed area of the AIE-active substrate and the PL intensity from the stretchable triboelectric-photonic smart skin (STPS), as shown in Fig. 9f. The Ag NW network in the middle served as a stretchable conductive layer. The AIE compound, bis(4-phenothiazinephenyl) sulfone, acted as a solid intensive fluorescent emitter. A crack occurred at the position where the finger was bent, thereby causing light to be emitted. Furthermore, the authors integrated the STPS onto the five fingers of a robot. As shown in Fig. 9g, when the gesture "OK" was made, the 3D distribution of the light signal and the luminescent photograph indicated the degree of bending of each finger [109].

Furthermore, the development of intelligent systems enables robots to have auditory sense and tactile sense. A circular-type single-channel self-powered triboelectric auditory sensor (TAS) was designed, which was used to construct an electronic auditory system and an external hearing aid for robots. A schematic diagram of the TAS is shown in Fig. 10a. The TAS was a circular device consisting of fluorinated ethylene propylene (FEP) plated with a top electrode and comprising a plurality of channels, as well as a Kapton film with a bottom electrode. A gap was formed in the middle so that the inside could freely vibrate. With the application of the TAS, sound could be used to turn on a console light and to trigger an antitheft system, as shown in Fig. 10b. Due to the structure of the triboelectric cochlea (TEC) device, it could be easily integrated into the artificial ears of robots. Fig. 10c shows the sound wave signal of original music and recorded music. The graph shows that the two sound wave signals were almost identical. Moreover, the voice recognition capabilities of the robot are demonstrated in Fig. 10d, e, which proves the feasibility of using the TAS in a robotic auditory system [112].

To achieve perception of multiple stimuli by a robot, Wang and Pan groups [14] presented a stretchable tactile sensor network of island-bridge structures, which was used to simulate human somatosensory systems, as shown in Fig. 10f. This network could detect temperature, relative humidity, magnetic field, in-plane strain, ultraviolet light, proximity and pressure. The perception of temperature and pressure is an important feature of human skin, so smart prosthetic hands have been designed that can be used to feel pressure and temperature. Fig. 10h shows the distribution of five tactile pressure sensors and tactile a temperature sensor on an intelligent prosthetic hand. Fig. 10g depicts the different responses of the smart prosthetic hand when grasping and releasing objects. At the same time, when the smart prosthetic hand grabbed a cup, it would make different inferences for different temperatures.

4. Conclusion and perspective

In this review, we introduced the rapid development of material technology, flexible electronics, and nanotechnology in the field of tactile sensors and their application in intelligent systems. Recent studies have demonstrated improvements in the resolution, sensitivity, and other properties of devices. Meanwhile, the designs of devices have become more reasonable and mature to provide multifunctionality, such as stretchability, self-healing, self-powered

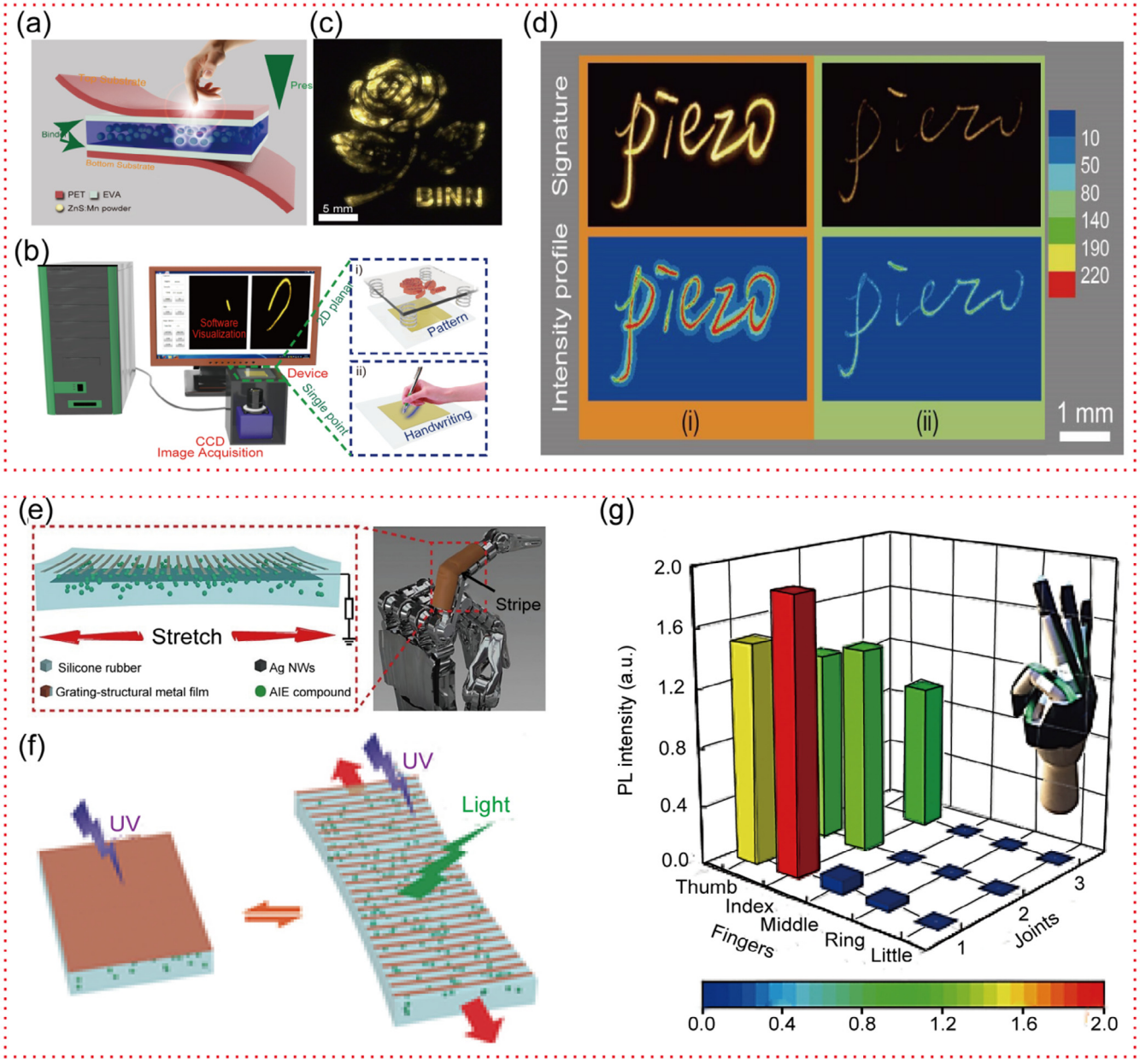

Fig. 9. (Color online) Application of tactile sensors in intelligent human–machine interfaces. (a) Schematic diagram of flexible tactile pressure sensors for an electronic signature system. (b) Schematic diagram of an image acquisition and processing system for two-dimensional plane and single-point dynamic pressure. (c) Rose pattern produced by pressing a stamp on the device. (d) Different signers showed different signature habits. Reprinted with permission from Ref. [108], Copyright © 2015 Wiley-VCH. (e) Schematic diagram of a tactile sensor that senses external stimuli and gestures. (f) Schematic diagram of the photoluminescence principle of devices based on grating structure metal thin films. (g) 3D normalized PL intensity map of the gesture "OK". Reprinted with permission from Ref. [109], Copyright © 2018 Wiley-VCH.

capability and biodegradability. Thus, the development of tactile sensors provides a platform for wearable devices, biomedical systems, man–machine interaction systems and intelligent robots, which pushes the development of intelligent systems.

However, tactile sensors still face enormous challenges in practical applications. First, the performance of tactile sensors, such as the sensitivity and flexibility, is still the main research field. With the application of surface micromachining technology, researchers can develop tactile sensors from tactile arrays to high-density arrays to increase the resolution and sensitivity. In addition to the development tendency mentioned above, the use of piezoelectric nanowires can realize high resolution and low crosstalk between pixels, and on this basis, the introduction of TENGs can enable a device with low power consumption and high sensitivity. Elastomeric materials and stretchable structures have also successfully expanded the effective sensing area of devices. PENGs and TENGs have been proposed to enable devices with a self-powered capability. With the study of self-healing materials and biodegradable materials, tactile sensors are becoming increasingly widely used in intelligent systems and provide a simpler and safer development direction for wearable devices, implantable devices and so on. Meeting these challenges will bring new opportunities. Second, sensors undergo repeated deformation during actual use, and the deformations will affect the performance of devices. Therefore, the detection accuracy and lifetimes of devices are seriously reduced. Researchers can make greater efforts in realizing advanced materials and suitable structures to improve the durability of devices. At the same time, the development of packaging

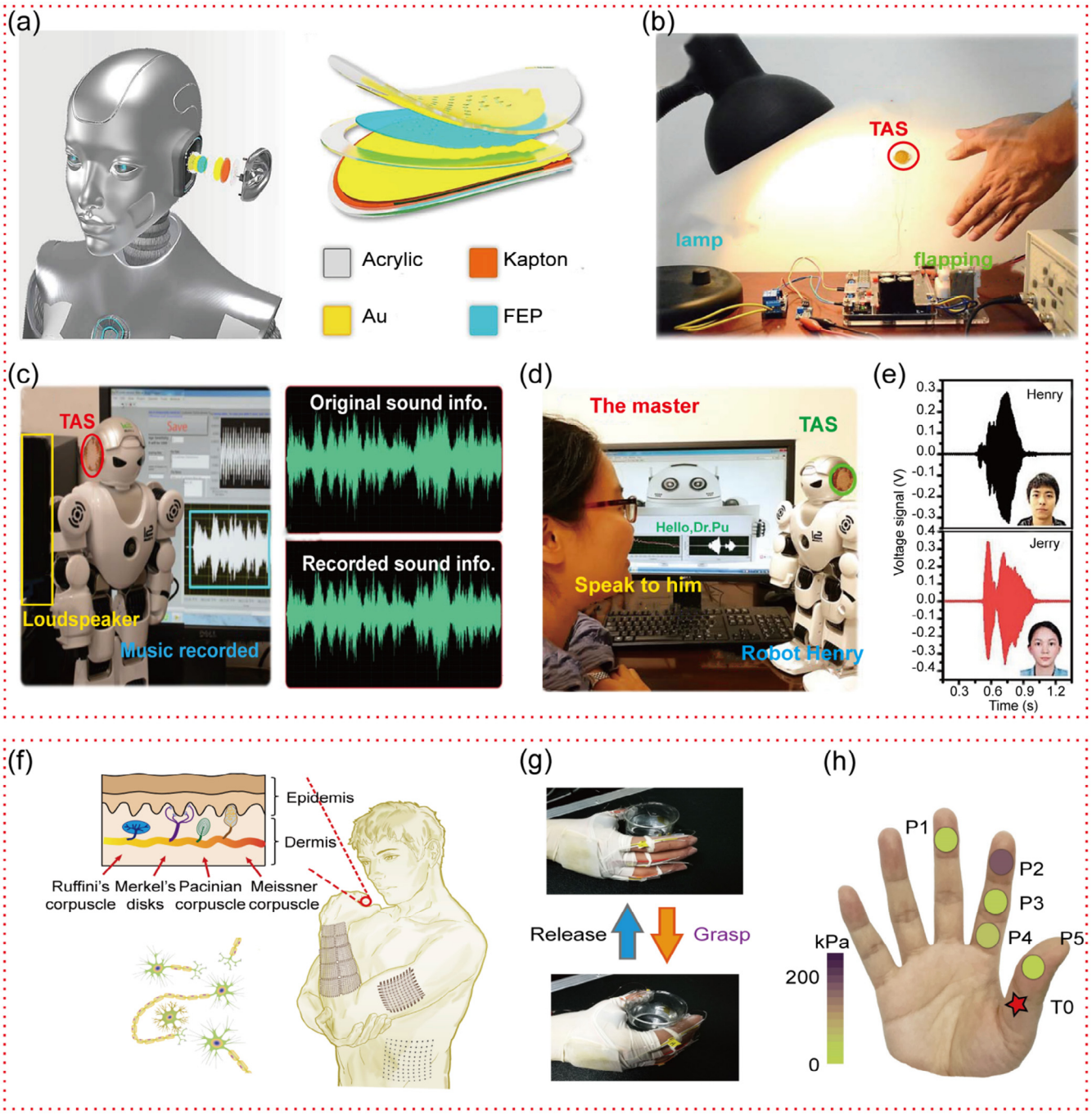

Fig. 10. (Color online) Application of auditory and tactile sensors in intelligent systems. (a) Schematic diagram of a robot's auditory sensor. (b) Demonstration of the device as a voice-activated switch. (c) The waveform of the original music was roughly the same as that of the music recorded by the robotic auditory system. (d) Demonstration of the device as a voice recognition system. (e) Different timbres produced different waveforms. Reprinted with permission from Ref. [112], Copyright © 2018 AAAS. (f) Schematic diagram of multisensory electronic skin. (g) Schematic diagram of the operation of an intelligent prosthetic hand to grasp and release a cup. (h) Distribution of five tactile pressure sensors and a tactile temperature sensor on the intelligent prosthetic hand. Reprinted with permission from Ref. [14], Copyright © 2018 Springer Nature.

materials and packaging technology is another important way to improve the stability and durability of devices. Third, in practical applications, multiple stimuli tend to occur in the same place at the same time. To achieve the detection of all stimuli, decoupling of crosstalk signals of tactile sensors is required. The simultaneous collection of multiple signals with no crosstalk is important and is of great significance to developing new tactile sensors that can be applied in intelligent systems. In addition, the integration of the sensing system also imposes requirements on the components. Each component of tactile sensors in an intelligent system must have mechanical, optical, electrical and thermal property matching. Meeting these challenges will bring new opportunities. The tactile sensors used in intelligent systems will be flexible, miniature, and multifunctional.

Conflict of interest

The authors declare that they have no conflict of interest.

Acknowledgments

This work was supported by the National Key Research and Development Program of China (2016YFA0202703), the National Natural Science Foundation of China (51622205, 61675027, 51432005, 61505010, and 51502018), Beijing City Committee of Science and Technology (Z171100002017019 and Z181100004418004), and Beijing Natural Science Foundation (4181004, 4182080, 4184110, and 2184131).

Author contributions

Yue Liu, Rongrong Bao, Juan Tao, and Caofeng Pan carried out the concepts, design, definition of intellectual content, literature search and manuscript preparation. Jing Li and Ming Dong provided assistance for literature search, data acquisition and statistical analysis. Yue Liu, Rongrong Bao, and Caofeng Pan carried out manuscript editing. All authors have read and approved the content of the manuscript.

References

[1] Malcolm AB. The development and application of novel intelligent scoring systems in critical illness. In: Proceedings of the Iaea Spent Fuel Conference June; 2015.
[2] Gao ZD, Su JB, Zhou W. Robot autonomous perception model for internet. In: Proceedings of the International Conference on Machine Learning & Cybernetics; 2005.
[3] Pinna L, Ibrahim A, Valle M. Interface electronics for tactile sensors based on piezoelectric polymers. IEEE Sens J 2017;17:5937–47.
[4] Hidalgo-Lopez JA, Oballe-Peinado O, Castellanos-Ramos J, et al. High-accuracy readout electronics for piezoresistive tactile sensors. Sensors 2017;17:2513.
[5] Pugach G, Khomenko V, Melnyk A, et al. Electronic hardware design of a low cost tactile sensor device for physical human-robot interactions. 2013 IEEE Xxxiii International Scientific Conference Electronics and Nanotechnology (Elnano), 2013, 445–449.
[6] Rocha JG, Santos C, Cabral JM, et al. 3 Axis capacitive tactile sensor and readout electronics. 2006. IEEE Int Sympos Indust Electron 2006;1–7:2767.
[7] Hsiung YS, Lu SC. A CMOS capacitive pressure sensor chip for fingerprint detection. In: Proceedings of the Solid-state Sensors, Actuators & Microsystems Conference; 2011.
[8] Dargahi J, Najarian S. Human tactile perception as a standard for artificial tactile sensing–a review. Int J Med Robot Comput Assist Surg 2004;1:23–35.
[9] Damiani E, Jain LC, Howlett RJ. Knowledge-based intelligent information engineering. KES 2002 Systems and Allied Technologies; 2003.
[10] Yang T, Xie D, Li Z, et al. Recent advances in wearable tactile sensors: Materials, sensing mechanisms, and device performance. Mater Sci Eng R 2017;115:1–37.
[11] Wang X, Zhang SR, Dong L, et al. Self-powered high-resolution and pressure-sensitive triboelectric sensor matrix for real-time tactile mapping. Adv Mater 2016;28:2896–903.
[12] Wei XY, Wang X, Kuang SY, et al. Dynamic triboelectrification-induced electroluminescence and its use in visualized sensing. Adv Mater 2016;28:6656–64.
[13] Wang X, Zhang Y, Zhang X, et al. A highly stretchable transparent self-powered triboelectric tactile sensor with metallized nanofibers for wearable electronics. Adv Mater 2018;30:e1706738.
[14] Hua Q, Sun J, Liu H, et al. Skin-inspired highly stretchable and conformable matrix networks for multifunctional sensing. Nat Commun 2018;9:244.
[15] Wang S, Xu J, Wang W, et al. Skin electronics from scalable fabrication of an intrinsically stretchable transistor array. Nature 2018;555:83–8.
[16] Tee BC, Wang C, Allen R, et al. An electrically and mechanically self-healing composite with pressure- and flexion-sensitive properties for electronic skin applications. Nat Nanotechnol 2012;7:825–32.
[17] Sun J, Pu X, Liu M, et al. Self-healable, stretchable, transparent triboelectric nanogenerators as soft power sources. ACS Nano 2018;12:6147–55.
[18] Wang X, Que C, Chen M, et al. Full dynamic-range pressure sensor matrix based on optical and electrical dual-mode sensing. Adv Mater 2017;29:1605817.
[19] Dudem B, Mule AR, Patnam HR, et al. Wearable and durable triboelectric nanogenerators via polyaniline coated cotton textiles as a movement sensor and self-powered system. Nano Energy 2019;55:305–15.
[20] Hwang SW, Tao H, Kim DH, et al. A physically transient form of silicon electronics. Science 2012;337:1640–4.
[21] Boutry CM, Beker L, Kaizawa Y, et al. Biodegradable and flexible arterial-pulse sensor for the wireless monitoring of blood flow. Nat Biomed Eng 2019;3:47.
[22] Kang SK, Murphy RK, Hwang SW, et al. Bioresorbable silicon electronic sensors for the brain. Nature 2016;530:71.
[23] Lei T, Guan M, Liu J, et al. Biocompatible and totally disintegrable semiconducting polymer for ultrathin and ultralightweight transient electronics. Proc Natl Acad Sci USA 2017;114:5107–12.
[24] Chen N, Rink R, Zhang H. Efficient edge detection from tactile data. Iros '95 – 1995 IEEE/Rsj International Conference on Intelligent Robots and Systems: Human Robot Interaction and Cooperative Robots, Proceedings, 1995, 3: 386–391.
[25] Lee JS, Shin KY, Cheong OJ, et al. Highly sensitive and multifunctional tactile sensor using free-standing ZnO/PVDF thin film with graphene electrodes for pressure and temperature monitoring. Sci Rep 2015;5:7887.
[26] Guo H, Chen J, Tian L, et al. Airflow-induced triboelectric nanogenerator as a self-powered sensor for detecting humidity and airflow rate. ACS Appl Mater Interfaces 2014;6:17184–9.
[27] Chen S, Jiang K, Lou Z, et al. Recent developments in graphene-based tactile sensors and e-skins. Adv Mater Technol 2018;3:1700248.
[28] Qin L, Zhang Y. Roughness discrimination with bio-inspired tactile sensor manually sliding on polished surfaces. Sens Actuator A Phys 2018;279:433–41.
[29] Hattori Y, Falgout L, Lee W, et al. Multifunctional skin-like electronics for quantitative, clinical monitoring of cutaneous wound healing. Adv Healthc Mater 2014;3:1597–607.
[30] Chi C, Sun X, Xue N, et al. Recent progress in technologies for tactile sensors. Sensors. Sensors 2018;18:948.
[31] Benight SJ, Wang C, Tok JBH, et al. Stretchable and self-healing polymers and devices for electronic skin. Prog Polym Sci 2013;38:1961–77.
[32] Wang ZL. Progress in piezotronics and piezo-phototronics. Adv Mater 2012;24:4632–46.
[33] Liu S, Wang L, Feng X, et al. Ultrasensitive 2D ZnO peizotronic transistor array for high resolution tactile imaging. Adv Mater 2017;29:1606346.
[34] Zhao X, Hua Q, Yu R, et al. Flexible, stretchable and wearable multifunctional sesor array as artificial electronic skin for static and dynamic strain mapping. Adv Electron Mater 2015;1:1500142.
[35] Wang Y, Gong S, Schwalb W, et al. A wearable and highly sensitive pressure sensor with ultrathin gold nanowires. Nat Commun 2014;5:3132.
[36] Martinez-Hernandez U. Tactile sensors. In: Scholarpedia of touch. Berlin: Springer 2016:783–96.
[37] Chen N, Rink R, Zhang H, et al. Efficient edge detection from tactile data. . Iros '95 – 1995 IEEE/Rsj International Conference on Intelligent Robots and Systems: Human Robot Interaction and Cooperative Robots, Proceedings 1995;3:386–91.
[38] Takashima K, Horie S, Mukai T, et al. Piezoelectric properties of vinylidene fluoride oligomer for use in medical tactile sensor applications. Sens Actuat A Phys 2008;144:90–6.
[39] Calisti M, Corucci F, Arienti A, et al. Dynamics of underwater legged locomotion: modeling and experiments on an octopus-inspired robot. Bioinspir Biomim 2015;10:46012.
[40] Pang C, Kim TI, Bae WG, et al. Bioinspired reversible interlocker using regularly arrayed high aspect-ratio polymer fibers. Adv Mater 2012;24:475–9.
[41] Akhras G. Smart materials and smart systems for the future. Canadian Military J 2000;1:25–31.
[42] Wang ZL. Piezopotential gated nanowire devices: piezotronics and piezo-phototronics. Nano Today 2010;5:540–52.
[43] Schmidt PA, Maël E, Würtz RP. A sensor for dynamic tactile information with applications in human–robot interaction and object exploration. Robot Auton Syst 2006;54:1005–14.
[44] Wu WZ, Wen XN, Wang ZL. Taxel-addressable matrix of vertical-nanowire piezotronic transistors for active and adaptive tactile imaging. Science 2013;340:952–7.
[45] Pan C, Dong L, Zhu G, et al. High-resolution electroluminescent imaging of pressure distribution using a piezoelectric nanowire led array. Nat Photonics 2013;7:752–8.
[46] Bao R, Wang C, Dong L, et al. Flexible and controllable piezo-phototronic pressure mapping sensor matrix by ZnO NW/p-polymer LED array. Adv Funct Mater 2015;25:2884–91.
[47] Bao R, Wang C, Dong L, et al. CdS nanorods/organic hybrid LED array and the piezo-phototronic effect of the device for pressure mapping. Nanoscale 2016;8:8078–82.
[48] Bao R, Wang C, Peng Z, et al. Light-emission enhancement in a flexible and size-controllable ZnO nanowire/organic light-emitting diode array by the piezotronic effect. ACS Photon 2017;4:1344–9.
[49] Bao R, Li J, Tao J, et al. Recent progress in flexible pressure sensor arrays: from design to applications. J Mater Chem C 2018;6:11878–92.
[50] Peng Y, Que M, Lee HE, et al. Achieving high-resolution pressure mapping via flexible GAN/ZnO nanowire leds array by piezo-phototronic effect. Nano Energy 2019;58:633–40.
[51] Du L, Zhang Y, Lei Y, et al. Synthesis of high-quality CDS nanowires and their application as humidity sensors. Mater Lett 2014;129:46–9.
[52] Zhou D, Wang H. Design and evaluation of a skin-like sensor with high stretchability for contact pressure measurement. Sens Actuat A Phys 2013;204:114–21.
[53] Hong S, Lee H, Lee J, et al. Highly stretchable and transparent metal nanowire heater for wearable electronics applications. Adv Mater 2015;27:4744–51.
[54] Hou C, Xu Z, Qiu W, et al. A biodegradable and stretchable protein-based sensor as artificial electronic skin for human motion detection. Small 2019;15:1805084

[55] Cheng Y, Wang R, Zhai H, et al. Stretchable electronic skin based on silver nanowire composite fiber electrodes for sensing pressure, proximity, and multidirectional strain. Nanoscale 2017;9:3834–42.
[56] Cao Y, Zhang G, Zhang Y, et al. Direct fabrication of stretchable electronics on a polymer substrate with process-integrated programmable rigidity. Adv Funct Mater 2018;28:1804604.
[57] Urban MW. Stratification, stimuli-responsiveness, self-healing, and signaling in polymer networks. Prog Polym Sci 2009;34:679–87.
[58] Wong TS, Kang SH, Tang SK, et al. Bioinspired self-repairing slippery surfaces with pressure-stable omniphobicity. Nature 2011;477:443–7.
[59] Rao YL, Chortos A, Pfattner R, et al. Stretchable self-healing polymeric dielectrics cross-linked through metal-ligand coordination. J Am Chem Soc 2016;138:6020–7.
[60] Hohlbein N, Shaaban A, Schmidt AM. Remote-controlled activation of self-healing behavior in magneto-responsive ionomeric composites. Polymer 2015;69:301–9.
[61] Herbst F, Dohler D, Michael P, et al. Self-healing polymers via supramolecular forces. Macromol Rapid Commun 2013;34:203–20.
[62] Hart LR, Nguyen NA, Harries JL, et al. Perylene as an electron-rich moiety in healable, complementary π–π stacked, supramolecular polymer systems. Polymer 2015;69:293–300.
[63] Yang Y, Urban MW. Self-healing polymeric materials. Chem Soc Rev 2013;42:7446–67.
[64] Kaes C, Katz A, Hosseini MW. Bipyridine: the most widely used ligand. A review of molecules comprising at least two 2,2'-bipyridine units. Cheminform 2000;31:3553–90.
[65] Zhu G, Peng B, Chen J, et al. Triboelectric nanogenerators as a new energy technology: from fundamentals, devices, to applications. Nano Energy 2015;14:126–38.
[66] Guo W, Zhang X, Yu R, et al. CoS NWs/Au hybridized networks as efficient counter electrodes for flexible sensitized solar cells. Adv Energy Mater 2015;5:1500141.
[67] Hu G, Guo W, Yu R, et al. Enhanced performances of flexible ZnO/perovskite solar cells by piezo-phototronic effect. Nano Energy 2016;23:27–33.
[68] Kang TJ, Fang S, Kozlov ME, et al. Electrical power from nanotube and graphene electrochemical thermal energy harvesters. Adv Funct Mater 2012;22:477–89.
[69] Fan FR, Tang W, Wang ZL. Flexible nanogenerators for energy harvesting and self-powered electronics. Adv Mater 2016;28:4283–305.
[70] Wang ZL, Zhu G, Yang Y, et al. Progress in nanogenerators for portable electronics. Mater Today 2012;15:532–43.
[71] Wang ZL, Song JH. Piezoelectric nanogenerators based on zinc oxide nanowire arrays. Science 2006;312:242–6.
[72] Shi K, Huang X, Sun B, et al. Cellulose/$BaTiO_3$ aerogel paper based flexible piezoelectric nanogenerators and the electric coupling with triboelectricity. Nano Energy 2019;57:450–8.
[73] Chen J, Oh SK, Nabulsi N, et al. Biocompatible and sustainable power supply for self-powered wearable and implantable electronics using iii-nitride thin-film-based flexible piezoelectric generator. Nano Energy 2019;57:670–9.
[74] Fan FR, Tian ZQ, Wang ZL. Flexible triboelectric generator. Nano Energy 2012;1:328–34.
[75] Wang ZL. On Maxwell's displacement current for energy and sensors: the origin of nanogenerators. Mater Today 2017;20:74–82.
[76] Tao J, Bao R, Wang X, et al. Self-powered tactile sensor array systems based on the triboelectric effect. Adv Funct Mater 2018;29:1806379.
[77] Jeon YP, Park JH, Kim TW. Highly flexible triboelectric nanogenerators fabricated utilizing active layers with a ZnO nanostructure on polyethylene naphthalate substrates. Appl Surf Sci 2019;466:210–4.
[78] Cheedarala RK, Parvez AN, Ahn KK. Electric impulse spring-assisted contact separation mode triboelectric nanogenerator fabricated from polyaniline emeraldine salt and woven carbon fibers. Nano Energy 2018;53:362–72.
[79] Zhang C, Li J, Han CB, et al. Organic tribotronic transistor for contact-electrification-gated light-emitting diode. Adv Funct Mater 2015;25:5625–32.
[80] Zhao G, Zhang X, Cui X, et al. Piezoelectric polyacrylonitrile nanofiber film-based dual-function self-powered flexible sensor. ACS Appl Mater Interfaces 2018;10:15855–63.
[81] Fang H, Wang X, Li Q, et al. A stretchable nanogenerator with electric/light dual-mode energy conversion. Adv Energy Mater 2016;6:1600829.
[82] Amin R, Islam SKH, Biswas GP, et al. A robust and anonymous patient monitoring system using wireless medical sensor networks. Futur Gener Comp Syst 2018;80:483–95.
[83] Shnayder V, Chen B, Lorincz K, et al. Sensor networks for medical care. Boston: Harvard University, 2005.
[84] So Hwang, Kim D, Hu T, et al. Materials and fabrication processes for transient and bioresorbable high-performance electronics. Adv Funct Mater 2013;23:4087–93.
[85] Canan D, Suk-Won H, Yewang S, et al. Transient, biocompatible electronics and energy harvesters based on ZnO. Small 2013;9:3398–404.
[86] Irimia-Vladu M. "Green" electronics: biodegradable and biocompatible materials and devices for sustainable future. Chem Soc Rev 2014;43:588–610.
[87] Henson ZB, Mullen K, Bazan GC. Design strategies for organic semiconductors beyond the molecular formula. Nat Chem 2012;4:699–704.
[88] Jiang W, Li H, Liu Z, et al. Fully bioabsorbable natural-materials-based triboelectric nanogenerators. Adv Mater 2018;30:1801895
[89] Li Z, Feng H, Zheng Q, et al. Photothermally tunable biodegradation of implantable triboelectric nanogenerators for tissue repairing. Nano Energy 2018;54:390–9.
[90] Oh JY, Rondeau-Gagné S, Chiu YC, et al. Intrinsically stretchable and healable semiconducting polymer for organic transistors. Nature 2016;539:411.
[91] Castillejo P, Martinez JF, Rodriguez-Molina J, et al. Integration of wearable devices in a wireless sensor network for an e-health application. IEEE Wirel Commun 2013;20:6590049.
[92] Chang IC, Hwang HG, Hung MC, et al. Factors affecting the adoption of electronic signature: executives' perspective of hospital information department. Decis Support Syst 2007;44:350–9.
[93] Ha M, Lim S, Ko H. Wearable and flexible sensors for user-interactive health-monitoring devices. J Mater Chemi B 2018;6:4043–64.
[94] Liu Z, Zhang S, Jin YM, et al. Flexible piezoelectric nanogenerator in wearable self-powered active sensor for respiration and healthcare monitoring. Semicond Sci Technol 2017;32:064004
[95] Uğur S. Wearing embodied emotions: a practice based design research on wearable technology. Berlin: Springer; 2013.
[96] Jeong SM, Song S, Seo HJ, et al. Battery-free, human-motion-powered light-emitting fabric: Mechanoluminescent textile. Adv Sustain Syst 2017;1:1700126.
[97] Zhang Z, Cui L, Shi X, et al. Textile display for electronic and brain-interfaced communications. Adv Mater 2018;30:e1800323.
[98] O'Connor B, An KH, Zhao Y, et al. Fiber shaped light emitting device. Adv Mater 2007;19:3897–900.
[99] Leahy MJ, Henry MP, Clarke DW. Sensor validation in biomedical applications. Control Eng Practice 1997;5:1753–8.
[100] Tiwana MI, Redmond SJ, Lovell NH. A review of tactile sensing technologies with applications in biomedical engineering. Sens Actuat A Phys 2012;179:17–31.
[101] Afshari E, Najarian S, Simforoosh N, et al. Evaluation of a new method for detection of kidney stone during laparoscopy using 3D conceptual modeling. Int J Med Medical Sci 2010;1:56–61.
[102] Cao X, Halder A, Tang Y, et al. Engineering two-dimensional layered nanomaterials for wearable biomedical sensors and power devices. Mater Chem Front 2018;2:1944–86.
[103] Ouyang H, Tian J, Sun G, et al. Self-powered pulse sensor for antidiastole of cardiovascular disease. Adv Mater 2017;29:1703456
[104] Liu Z, Ma Y, Ouyang H, et al. Transcatheter self-powered ultrasensitive endocardial pressure sensor. Adv Funct Mater 2019;29:1807560.
[105] Wang G, Feng H, Hu L, et al. An antibacterial platform based on capacitive carbon- doped TiO_2 nanotubes after direct or alternating current charging. Nat Commun 2018;9:2055.
[106] Hall SA, Cigarroa CG, Marcoux L, et al. Time course of improvement in left ventricular function, mass and geometry in patients with congestive heart failure treated with beta-adrenergic blockade. J Am Coll Cardiol 1995;25:1154–61.
[107] Jaimes A, Sebe N. Multimodal human-computer interaction: a survey. Comput Vision Image Understanding, 2007, 108: 116–134.
[108] Wang X, Zhang H, Yu R, et al. Dynamic pressure mapping of personalized handwriting by a flexible sensor matrix based on the mechanoluminescence process. Adv Mater 2015;27:2324–31.
[109] Bu T, Xiao T, Yang Z, et al. Stretchable triboelectric-photonic smart skin for tactile and gesture sensing. Adv Mater 2018;30:e1800066.
[110] Wang W, Zhang H, Peng D, et al. Mechanically induced light emission and infrared- laser-induced upconversion in the Er-doped caznos multifunctional piezoelectric semiconductor for optical pressure and temperature sensing. J Phys Chem C 2015;119:28136–42.
[111] Wang W, Peng D, Zhang H, et al. Mechanically induced strong red emission in samarium ions doped piezoelectric semiconductor caznos for dynamic pressure sensing and imaging. Opt Commun 2017;395:24–8.
[112] Guo HY, Pu XJ, Chen J, et al. A highly sensitive, self-powered triboelectric auditory sensor for social robotics and hearing aids. Sci Robot 2018;3: UNSP: eaat2516.

Yue Liu received her B.S. degree from the China University of Geosciences (Beijing) in 2017. She is currently a Master's student with Prof. Caofeng Pan at Beijing Institute of Nanoenergy and Nanosystems, Chinese Academy of Sciences. Her current research interests focus on flexible pressure sensor devices and their applications in human-machine interfaces.

Rongrong Bao received her B.S. degree from Tianjin University in 2007 and Ph.D. degree from Technical Institute of Physics and Chemistry, Chinese Academy of Science (CAS) in 2012. She was a postdoc fellow in the same institute. She has been an Associate Professor in the group of Prof. Caofeng Pan at Beijing Institute of Nanoenergy and Nanosystems, CAS since 2016. Her main research interests focus on the fields of the production and characterization of organic-inorganic composite nanodevices and flexible pressure sensors.

Caofeng Pan received his B.Sc. degree (2005) and Ph.D. (2010) degree in Materials Science and Engineering from Tsinghua University, China. Then, he joined the group of Prof. Zhong Lin Wang at the Georgia Institute of Technology as a postdoctoral fellow. He has been a professor and a group leader at the Beijing Institute of Nanoenergy and Nanosystems, Chinese Academy of Sciences since 2013. His research interests mainly focus on the fields of piezotronics/piezo-phototronics for fabricating new electronic and optoelectronic devices, nanopower sources, hybrid nanogenerators, and self-powered nanosystems.